Scientia Iranica (2024) 31(15), 1293–1312

Sharif University of Technology
Scientia Iranica
Transactions E: Industrial Engineering
https://scientiairanica.sharif.edu

Monitoring coefficient of variation using variable sampling interval double exponentially weighted moving average charts

X.L. Hu[a,*], S.Y. Zhang[b], Y. Zhang[c], J.J. Zhang[d], and P.P. Zhou[e]

a. *Institute of High-Quality Development Evaluation, Nanjing University of Posts and Telecommunications, Nanjing, China.*
b. *School of Management, Nanjing University of Posts and Telecommunications, Nanjing, China.*
c. *School of Management, Tianjin University of Commerce, Tianjin, China.*
d. *Department of Mathematics, Liaoning University, Shenyang, China.*
e. *School of Management Science and Engineering, Nanjing University of Finance and Economics, Nanjing, China.*

Received 29 June 2021; received in revised form 2 September 2021; accepted 25 October 2021

KEYWORDS
DEWMA chart;
Variable sampling interval;
Coefficient of variation;
Average time to signal;
EWMA chart.

Abstract. As a measure of relative variability, the Coefficient of Variation (CV) is a valuable charting statistic in statistical process control. Great efforts have been devoted to monitoring CV efficiently. To further improve the performance of CV charts, this paper proposes three Double Exponentially Weighted Moving Average (DEWMA) charts by incorporating Variable Sampling Interval (VSI) strategies to monitor the CV squared. The run length properties of the proposed charts are evaluated via Monte Carlo simulations. Comparative studies show that the proposed VSI DEWMA CV charts detect the process shifts faster than the existing CV charts. A real data example is presented to illustrate the VSI DEWMA CV charts.

1. Introduction

The control chart is one of the effective tools for monitoring and controlling a process in Statistical Process Control (SPC). Three types of most widely-used control charts are the Shewhart charts, the Exponentially Weighted Moving Average (EWMA) control charts and the Cumulative Sum (CUSUM) control charts. Among these charts, the Shewhart charts rely solely on the information of the current sample, and are efficient in detecting large shifts. By contrast, the EWMA and the CUSUM charts are superior in detecting small to moderate shifts by utilizing both the past and current sample information.

Many efforts have been devoted to detecting changes in the process mean or variance based on the assumption of constant mean and variance. In recent years, control chart schemes have been applied to wider domains, such as education, health care, and finance, where the process mean and standard deviation may vary from time to time, see Yeong et

*. *Corresponding author. Tel.: +86-15950567942*
E-mail addresses: hxl0419@hotmail.com (X.L. Hu); 3147775409@qq.com (S.Y. Zhang); yzhang@tjcu.edu.cn (Y. Zhang); zjjly790816@163.com (J.J. Zhang); zhoupanpan@tju.edu.cn (P.P. Zhou)

To cite this article:
X.L. Hu, S.Y. Zhang, Y. Zhang, J.J. Zhang, and P.P. Zhou "Monitoring coefficient of variation using variable sampling interval double exponentially weighted moving average charts", *Scientia Iranica* (2024), **31**(15), pp. 1293-1312
https://doi.org/10.24200/sci.2021.58623.5819

al. [1]. In some of these applications, the mean is expected to fluctuate and the standard deviation is proportional to the mean. Thus, it is inappropriate to directly monitor the mean or the standard deviation. Monitoring the Coefficient of Variation (CV), which is a dimensionless and normalized measure of dispersion, is a better choice. The CV is defined as the ratio of the standard deviation σ to the mean μ, denoted as $\gamma = \sigma/\mu$. A process is claimed to be in-control if it has a constant CV. Nowadays, the CV is widely used in many different fields. For example, in the field of finance, it is considered as a measure of the risk, by relating the volatility of the return on an asset to the expected value of the return. In the field of material engineering, some quality characteristics related to the physical properties of metal alloys or composite materials have a constant CV when the process is in-control. These properties usually have relations with the way atoms of a material diffuse into another.

Monitoring the CV was first introduced by Kang et al. [2], who proposed the Shewhart-γ control chart (denoted as SH-γ) to monitor the cyclosporine level in organ-transplantation procedures using rational subgroups. Thereafter, an increasing number of EWMA- and CUSUM-type control charts have been put forward to enhance the sensitivity of the CV charts to small shifts. Hong et al. [3] and Castagliola et al. [4] respectively suggested EWMA schemes to monitor the CV. The former one monitored the CV using two-sided charts (EWMA-γ) with time-varying control limits, while the later one constructed two one-sided EWMA charts to monitor the CV squared (EWMA-γ^2) with constant control limits. Results of numerical experiments showed that the EWMA-γ^2 chart is superior to the EWMA-γ chart based on the Average Run Length (ARL). Calzada and Scariano [5] developed a synthetic CV chart and showed it performs better than the SH-γ chart but is inferior to the EWMA-γ^2 chart in detecting moderate upward shifts. Zhang et al. [6] improved the EWMA-γ^2 charts for detecting small shifts by modifying the charting statistic to incorporate all the samples information. Zhang et al. [7] enhanced the performance of the EWMA-γ^2 chart in detecting moderate and large shifts by integrating the resetting strategy proposed by Shu and Jiang [8]. Haq and Khoo [9] developed Adaptive Exponentially Weighted Moving Average (AEWMA) control charts for monitoring both univariate and multivariate CV and showed their significant advantages in detecting moderate to large shifts. Other studies including CV charts with run rules in Castagliola et al. [10], generally weighted moving average CV charts in Chen et al. [11], and run-sum CV charts in Teoh et al. [12] can be found. Recently Hu et al. [13] applied several Double Exponentially Weighted Moving Average (DEWMA) schemes to monitor the CV squared in order to further increase the sensitivity of the EWMA CV chart to small shifts in the process. The numerical analysis demonstrated that the proposed one-sided DEWMA $-\gamma^2$ charts always have a better performance than the competing charts when the shift is very small. A more comprehensive review on monitoring CV can be referred to Jalilibal et al. [14].

It is a common practice to draw samples of fixed sizes from the process within a Fixed Sampling Interval (FSI). In order to have a better understanding of the current process, however, it is necessary to take a larger number of samples in a shorter sampling interval when the process tends to be out-of-control. On the contrary, when the charting statistics are far away from the control limits, drawing samples of smaller sizes less frequently can save costs without increasing the out-of-control risk. Hence, adaptive control charts, the parameters of which vary with the samples, have attracted considerable research interest. The Variable Sample Size (VSS) charts and the Variable Sampling Interval (VSI) charts are the two main categories of adaptive control charts. Saccucci et al. [15] evaluated the Average Time to Signal (ATS) of two-sided VSI EWMA chart and concluded that the VSI EWMA chart is more efficient than the corresponding FSI EWMA chart. Shamma et al. [16] proposed a VSI DEWMA chart for detecting shifts in the process mean. The results showed that the VSI procedure performs better than the FSI DEWMA chart and reduces the number of switches between the sampling intervals compared to the VSI EWMA chart. Castagliola et al. [17] developed a VSS EWMA chart to monitor the sample variance and it was shown the chart outperforms the Fixed Sample Size and Interval (FSSI) chart. More examples of researches on VSI or VSS charts include Haq and Akhtar [18], Reynolds et al. [19] and Reynolds and Arnold [20], among others. In addition, some researchers applied the VSS or VSI features to enhance the performance of the traditional CV charts (see, [1,21–25]). In general, the charts with VSI or VSS strategies can detect the process shift earlier than the traditional charts.

In the light of the above literature review, this paper incorporates the VSI features to the three FSI DEWMA-γ^2 charts proposed by Hu et al. [13] so as to further improve their performances. The rest of this paper is organized as follows. The basic properties of the sample CV are described in Section 2, where the existing EWMA-γ^2 and DEWMA-γ^2 charts are also briefly reviewed. The DEWMA-γ^2 charts with VSI features are constructed in Section 3. Performances of the VSI DEWMA-γ^2 charts, the FSI DEWMA $-\gamma^2$ charts and the VSI EWMA-γ^2 charts are compared through Monte Carlo simulations in Section 4. Section 5 presents a real data application from the manufacturing process. Section 6 ends the paper with the summary of the main conclusions.

2. Some existing CV charts

This section provides the basis for the VSI DEWMA-γ^2 charts to be developed in Section 3. First, we describe the properties of the sample statistic CV. Then, we briefly introduce some existing CV charts, including the EWMA-γ^2 charts, the VSI EWMA-γ^2 charts and the three DEWMA-γ^2 charts proposed in Hu et al. [13].

2.1. Properties of the sample CV

Suppose that a manufacturing process yields the information of the subgroups $\{X_{k1}, X_{k2}, ..., X_{kn}\}$ of size n at each fixed time point $k = 1, 2, 3 \ldots$, where each $X_{k,i}, i = 1, 2, \ldots, n$ follows a normal distribution with mean μ_k and standard deviation σ_k. Furthermore, it is assumed that μ_k and σ_k are different from each subgroup. By definition, the sample CV $\hat{\gamma}_k$ of the process is defined as:

$$\hat{\gamma}_k = \frac{S_k}{\bar{X}_k},$$

where $\bar{X}_k$ and S_k are the sample mean and standard deviation, respectively, i.e:

$$\bar{X}_k = \frac{1}{n}\sum_{i=1}^{n} X_{ki},$$

and:

$$S_k = \sqrt{\frac{1}{n-1}\sum_{i=1}^{n}\left(X_{ki} - \bar{X}_k\right)^2}.$$

The distributional properties of the sample CV $\hat{\gamma}$ have been studied extensively. In order to monitor the CV squared, Castagliola et al. [4] deduced the distribution of the sample squared CV ($\hat{\gamma}^2$), and stated that $n/\hat{\gamma}^2$ has a noncentral F distribution with $(1, n-1)$ degrees of freedom and non-central parameter n/γ^2. The Cumulative Distribution Function (CDF) $F_{\hat{\gamma}^2}(x|n,\gamma)$ of $\hat{\gamma}^2$ and the Inverse Distribution Function (IDF) $F^{-1}_{\hat{\gamma}^2}(\alpha|n,\gamma)$ of $\hat{\gamma}^2$ are:

$$F_{\hat{\gamma}^2}(x|n,\gamma) = 1 - F_F\left(\frac{n}{x}|1, n-1, \frac{n}{\gamma^2}\right),$$

and:

$$F^{-1}_{\hat{\gamma}^2}(\alpha|n,\gamma) = \frac{n}{F_F^{-1}\left(1-\alpha|1, n-1, \frac{n}{\gamma^2}\right)},$$

where $F_F(.)$ is the CDF of the noncentral F distribution and $F_F^{-1}(.)$ is the IDF of the noncentral F distribution. Moreover, Breunig [26] investigated the mean $\mu_0(\hat{\gamma}^2)$ and the standard deviation $\sigma_0(\hat{\gamma}^2)$ of the CV squared with a bias correction method for inequality measures. The accurate approximations for $\mu_0(\hat{\gamma}^2)$ and $\sigma_0(\hat{\gamma}^2)$ are:

$$\mu_0\left(\hat{\gamma}^2\right) = \gamma_0^2\left(1 - \frac{3\gamma_0^2}{n}\right), \tag{1}$$

$$\sigma_0\left(\hat{\gamma}^2\right) = \left\{\gamma_0^4\left(\frac{2}{n-1} + \gamma_0^2\left(\frac{4}{n} + \frac{20}{n(n-1)} + \frac{75\gamma_0^2}{n^2}\right)\right) - \left(\mu_0\left(\hat{\gamma}^2\right) - \gamma_0^2\right)^2\right\}^{\frac{1}{2}}. \tag{2}$$

2.2. The existing EWMA-γ^2 chart without and with VSI features

2.2.1. The FSI EWMA-γ^2 chart

Considering the fact that monitoring S^2 rather than monitoring S is generally more efficient, Castagliola et al. [4] suggested monitoring γ^2 instead of γ. In addition, using two one-sided EWMA charts can overcome the inertia problem of the two-sided EWMA chart and the detection effectiveness of one-sided charts is better than that of two-sided charts. Therefore, the two one-sided EWMA-γ^2 charts were developed to improve the performance of the two-sided EWMA-γ chart in Hong et al. [3]. The upward EWMA-γ^2 chart for detecting an increase in the CV was suggested with the following charting statistic:

$$Z_k = \max\left(\mu_0\left(\hat{\gamma}^2\right), (1-\lambda) Z_{k-1} + \lambda\hat{\gamma}_k^2\right), \tag{3}$$

where $\lambda \in (0, 1]$ is the smoothing parameter and the initial value is $Z_0 = \mu_0(\hat{\gamma}^2)$. It is noted that Z_k is the maximum of the target value $\mu_0(\hat{\gamma}^2)$ and the traditional EWMA statistic $(1-\lambda) Z_{k-1} + \lambda\hat{\gamma}_k^2$. Whenever the traditional EWMA statistic is less than the target $\mu_0(\hat{\gamma}^2)$, Z_k is reset to $\mu_0(\hat{\gamma}^2)$. The upward chart triggers an out-of-control signal when Z_k is larger than the Upper Control Limit (UCL). The asymptotic UCL is computed as:

$$UCL = \mu_0\left(\hat{\gamma}^2\right) + K\sqrt{\frac{\lambda}{2-\lambda}}\sigma_0\left(\hat{\gamma}^2\right), \tag{4}$$

where K is the coefficient of the UCL. The ARL performance of the chart was computed using a Markov Chain method. The results showed that the EWMA-γ^2 chart yields a smaller ARL than the SH-γ chart and the EWMA-γ chart when the process is out-of-control.

2.2.2. The VSI EWMA-γ^2 chart

Following the work of Castagliola et al. [4], Yeong et al. [1] used the same Z_k in Eq. (3) as the charting statistic to construct a VSI EWMA-γ^2 chart. The UCL of the chart is the same as in Eq. (4). While the Upper Warning Limit (UWL) of the VSI EWMA-γ^2 chart is defined as:

$$UWL = \mu_0\left(\hat{\gamma}^2\right) + W\sqrt{\frac{\lambda}{2-\lambda}}\sigma_0\left(\hat{\gamma}^2\right), \tag{5}$$

where W is the coefficient of the UWL. When the statistics $Z_k \in [\mu_0\left(\hat{\gamma}^2\right), UWL]$, the process is declared as in-control and the next sample is taken after a long sampling interval h_l. If $Z_k \in [UWL, UCL]$, the process is considered to be still in-control but the next sample should be taken within a small sampling interval h_s. If Z_k exceeds the UCL, the process is declared as out-of-control and the potential assignable cause must be found and eliminated.

2.3. The DEWMA1-γ^2 chart

With the aim to further enhance the sensitivity to small shifts of CV charts, the traditional one-sided DEWMA chart in Shamma and Shamma [27] was employed to monitor the CV squared (denoted as DEWMA1-γ^2 chart). The upper-sided DEWMA1-γ^2 chart is defined as:

$$\begin{cases} Y_k = \lambda \hat{\gamma}_k^2 + (1-\lambda) Y_{k-1}, Y_0 = \mu_0\left(\hat{\gamma}^2\right) \\ Z_k = \lambda Y_k + (1-\lambda) Z_{k-1}, Z_0 = \mu_0\left(\hat{\gamma}^2\right) \end{cases}$$

where λ is the smoothing parameter. The asymptotic corresponding UCL is:

$$UCL = \mu_0\left(\hat{\gamma}^2\right) + K\sqrt{\frac{\lambda\left(2-2\lambda+\lambda^2\right)}{(2-\lambda)^3}}\sigma_0\left(\hat{\gamma}^2\right), \quad (6)$$

where the charting parameter K is selected to acquire the desired in-control ARL.

2.4. The DEWMA2-γ^2 chart

Similar to the method in Hamilton and Crowder [28], another DEWMA-γ^2 chart (denoted as DEWMA2-γ^2 chart) was constructed by resetting the traditional DEWMA statistics less than the target to the target by using the maximum function. This means that the statistic of the upper-sided DEWMA2-γ^2 chart is:

$$\begin{cases} Y_k = \lambda \hat{\gamma}_k^2 + (1-\lambda) Y_{k-1}, \\ \quad Y_0 = \mu_0\left(\hat{\gamma}^2\right), \\ Z_k = \max\left(\mu_0\left(\hat{\gamma}^2\right), \lambda Y_k + (1-\lambda) Z_{k-1}\right), \\ \quad Z_0 = \mu_0\left(\hat{\gamma}^2\right). \end{cases}$$

The corresponding asymptotic UCL of the upward DEWMA2-γ^2 chart is the same as in Eq. (6). When the statistics Z_k exceed the UCL, the process is declared to be out-of-control.

2.5. The DEWMA3-γ^2 chart

Shu and Jiang [8] developed another resetting technology by truncating the normalized observations below the target to the target. The third DEWMA-γ^2 chart (denoted as DEWMA3-γ^2 chart) was developed by adopting this strategy to monitor CV. First, normalize the current $\hat{\gamma}^2$ and then utilize the maximum function to reset the normalized $\hat{\gamma}^2$ to the target whenever it is less than the target, i.e:

$$W_k = \max\left(0, \frac{\hat{\gamma}_k^2 - \mu_0\left(\hat{\gamma}^2\right)}{\sigma_0\left(\hat{\gamma}^2\right)}\right).$$

Then, use the statistic W_k in the computation of the DEWMA recursion. As was shown in Zhang et al. [7],

$$\frac{\hat{\gamma}_k^2 - \mu_0\left(\hat{\gamma}^2\right)}{\sigma_0\left(\hat{\gamma}^2\right)},$$

approximately follows a standard normal distribution and, the mean and variance of W_k are:

$$E\left(W_k\right) = \frac{1}{\sqrt{2\pi}},$$

and

$$\sigma_{W_k}^2 = \frac{1}{2} - \frac{1}{2\pi}. \quad (7)$$

Based on the above analysis, the upward DEWMA3-γ^2 chart is constructed as:

$$\begin{cases} Y_k = \lambda\left(W_k - \frac{1}{\sqrt{2\pi}}\right) + (1-\lambda) Y_{k-1}, Y_0 = 0, \\ Z_k = \lambda Y_k + (1-\lambda) Z_{k-1}, Z_0 = 0. \end{cases}$$

This chart triggers an out-of-control signal when Z_k exceeds the UCL with:

$$UCL = K\sqrt{\frac{\lambda\left(2-2\lambda+\lambda^2\right)}{(2-\lambda)^3}}\sigma_{W_k}. \quad (8)$$

As has been shown in Hu et al. [13], among the three DEWMA-γ^2 charts, the DEWMA3-γ^2 chart has the best performance when the shift size is moderate to large. When the shift size is small, the chart is inferior to the other two DEWMA-γ^2 charts. The three DEWMA- γ^2 charts detect small shifts more efficiently than the EWMA-γ^2 chart, but they are relatively insensitive to moderate or large shifts compared with the EWMA-γ^2 chart. Hence, in the next section, we will integrate the VSI features into the three DEWMA-γ^2 charts to further improve the performance of the DEWMA CV charts in detecting small shifts and to enhance the charts' sensitivity to moderate and large shifts.

3. The proposed VSI DEWMA-γ^2 Charts

The CV charts presented above are mostly FSI schemes, except the VSI-EWMA-γ^2 chart in Yeong et al. [1]. Varying the sampling interval makes the process acquire samples quickly when there is a potential shift in the process, see Saccucci et al. [15]. In this section, the DEWMA-γ^2 charts with VSI features are proposed to further enhance the ability of the FSI DEWMA-γ^2 charts for monitoring the CV squared. For brevity, we mainly introduce the upper sided charts for the detection of upward shifts here. For the detection of downward shifts, the lower-sided charts are constructed in a similar manner.

Unlike the FSI scheme, the VSI scheme allows the chart to vary the time intervals between samples, depending on the current value of the charting statistic.

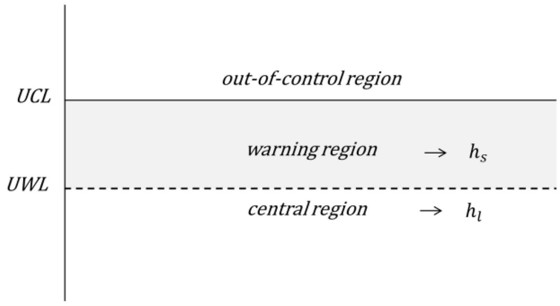

Figure 1. A graphical view of the upward Variable Sampling Interval (VSI) DEWMA-γ^2 charts.

According to the study of Saccucci et al. [15], two sampling intervals were suggested to keep the complexity of the VSI schemes at a reasonable level, i.e. $h_i \in \{h_s, h_l\}$, with h_s and h_l being the short and long sampling intervals, and to make a great progress in the chart's performance compared with the FSI charts. For the one-sided CV chart, by adding an UWL in the upward chart, the chart is divided into three regions, i.e., the central region, the warning region and the out-of-control region. Figure 1 is a graphical representation of the upward VSI DEWMA-γ^2 charts with an UWL added. If the value of charting statistic Z_k falls in the central region, i.e. $Z_k < UWL$, the process is claimed to be safe and waits for a long sampling interval h_l to get the next sample. If the value of the charting statistic Z_k lies in the warning region, i.e. $UWL \leq Z_k \leq UCL$, the process is at risk and is likely to be out-of-control. It would be wise to take the next sample within a short sampling interval h_s. If the statistic Z_k exceeds the UCL, the process is declared as out-of-control and some actions should be taken to find and eliminate the assignable causes as soon as possible.

When the process starts at time 0, there is no information available to decide which sampling interval should be used. In practice, it is common to take a short sampling interval as the first one to increase the sensitivity of the underlying control chart against the initial shifts in the CV. A general formula has been suggested by Reynolds et al. [19] to determine the values of h_s and h_l when the process is in-control. The formula is:

$$\begin{cases} \rho_1 h_s + \rho_2 h_l = 1, \\ \rho_1 + \rho_2 = 1, \end{cases} \tag{9}$$

where ρ_1 and ρ_2 are the probabilities of the charting statistic Z_k falling into the warning region and the central region, respectively, under the condition that no false alarm has occurred before.

- For the VSI DEWMA1-γ^2 chart and the VSI DEWMA2-γ^2 chart, the UCL in Eq. (4) is used and the UWL is defined as:

$$UWL = \mu_0\left(\hat{\gamma}^2\right) + W\sqrt{\frac{\lambda\left(2 - 2\lambda + \lambda^2\right)}{\left(2-\lambda\right)^3}}\sigma_0\left(\hat{\gamma}^2\right). \tag{10}$$

- For the VSI DEWMA3-γ^2 chart, the UCL is the same as in Eq. (8) in the FSI DEWMA3-γ^2 chart and the UWL of the chart is given as:

$$UWL = W\sqrt{\frac{\lambda\left(2 - 2\lambda + \lambda^2\right)}{\left(2-\lambda\right)^3}}\sigma_{W_k}. \tag{11}$$

In Eqs. (10) and (11), W is the coefficient of UWL of the corresponding VSI DEWMA-γ^2 charts. In the previous related research(see Haq and Akhtar [18]), a common choice is to take $h_s = 0.1$ and $h_l = 1.9$, which yields $\rho_1 = \rho_2 = 0.5$. Other combinations of $\{h_s, h_l\}$ and (ρ_1, ρ_2) can be adopted according to the specific needs of the practitioners. For simplicity, we only consider the case $(h_s, h_l) = (0.1, 1.9)$ and $\rho_1 = \rho_2 = 0.5$.

4. Numerical comparisons

ARL is a useful measure for evaluating and comparing performances of FSI control charts. For VSI charts, ATS is usually suggested since the interval between two successive samples is not constant. The ATS is defined as the expected time from the start of the process to the time when the chart signals. When the process is in-control, it is desirable to have a large in-control ATS (ATS_0), which indicates a low false alarm rate. If there is a shift in the process, it is expected to have an out-of-control ATS (ATS_0) as small as possible in order to timely detect an assignable cause.

For the FSI charts, the ATS is a multiple of the ARL due to the FSI, h, i.e., $ATS = ARL \times h$, where h is usually set to be one unit in practice. For the VSI charts, $ATS = ARL \times E(h_i)$, where $E(h_i)$ is the desired Average Sampling Intervals (ASI) of the VSI chart. To make a fair comparison between the FSI and VSI charts, the in-control ATS (ATS_0) of the VSI chart is set to be equal to the h of the FSI chart, i.e., ASI_0=1. At the same time, the ATS_0 of VSI chart should be consistent with the ATS_0 of the FSI chart. This constraint can be modeled as:

$$\begin{cases} ATS_0^{VSI} = ATS_0^{FSI}, \\ ASI_0^{VSI} = ASI_0^{FSI} = 1. \end{cases} \tag{12}$$

Without loss of generality, we assume $ATS_0 = 370.4$ in most simulations in this paper. Moreover, as suggested by the reviewer, we also study the performances of the FSI and VSI CV charts when $ATS_0 = 500$.

4.1. The simulation algorithm

The run length properties of CV control charts with FSI and VSI features are evaluated using Monte Carlo simulation method. When the process is in-control, the average number of samples (ATS_0/ASI_0) till the proposed one-sided VSI DEWMA-γ^2 chart triggers a false alarm is equal to that of the FSI one-sided DEWMA-γ^2 charts due to the constraint in Eq. (12). Therefore, the UCL values are the same for the FSI and VSI DEWMA–γ^2 charts. That is, the VSI DEWMA–γ^2 chart and the corresponding FSI DEWMA-γ^2 chart have the same parameter K. Moreover, a bisection search algorithm is used to find the coefficient W in the UWL of the VSI DEWMA-γ^2 chart to satisfy the Eq. (12). For illustration, the simplified steps to calculate the ATS values of the proposed VSI DEWMA-γ^2 charts are explained as follows:

1. Given in-control γ^2, the sample size n and a selected value of λ, use a bisection search algorithm to find the value of K in the UCL of the FSI DEWMA-γ^2 charts to satisfy the desired in-control ARL_0, i.e., $ARL_0 = 370.4$ in this paper. The details of the bisection search algorithm are given as follows:

   -Step 1. Set an appropriate interval $[K_L, K_U]$ of the parameter K, where K_L and K_U are the lower and the upper bounds, respectively;

   -Step 2. Choose a tolerance value Δ ($\Delta = 1$ in this paper) for the desired ARL_0;

   -Step 3. Compute the in-control ARL_P value corresponding to the parameter combination $(n, \lambda, K_P, \gamma_0)$, where $K_P = (K_L + K_U)/2$;

   -Step 4. If the calculated ARL_p in Step 3 is smaller than $ARL_0 - \Delta$, set $K_L = K_P$ and repeat Step 3; if ARL_p is larger than $ARL_0 + \Delta$, set $K_U = K_P$ and repeat Step 3. Stop when ARL_p falls in the interval $[ARL_0 - \Delta, ARL_0 + \Delta]$. Set the parameter $K = K_P$.

2. Find the value of W in the UWL of the VSI DEWMA-γ^2 charts that leads to $ATS_0^{VSI} = 370.4$ with the parameter combination $(n, \lambda, K, \gamma_0)$. Here, the above bisection algorithm is adopted to find W.

3. Based on the combination of $(n, \lambda, W, K, \gamma_0)$ found in Steps 1 and 2, the ATS_1 values of VSI DEWMA-γ^2 charts for different shifts are computed.

Following the research in Castagliola et al. [4], we set $n = 5$ and $\gamma_0 = \{0.05, 0.1, 0.15, 0.2\}$ here. Moreover, we set the smoothing parameters $\lambda = \{0.1, 0.2, 0.25, 0.3, 0.5\}$ and the shift sizes $\tau = \{1.05, 1.08, 1.1, 1.12, 1.15, 1.18, 1.2, 1.25, 1.5, 2\}$ for sensitivity analysis. Tables 1–5 (Columns 3 and 4) present the corresponding parameters W and K of the existing FSI and VSI EWMA-γ^2 charts and three DEWMA-γ^2 charts with and without the VSI features. The out-of-control values of these CV charts are computed for different values of τ (see columns 5 to 15 in Tables 1–5). The smallest ATS_1 values among these control charts are in bold in these tables.

4.2. Performance comparison of the proposed VSI DEWMA-γ^2 charts and the corresponding FSI DEWMA-γ^2 charts

From Tables 1–4, it can be seen that whatever the values of γ_0, λ and τ are, the VSI DEWMA-γ^2 charts always yield smaller ATS_1 values than the ones of the corresponding FSI DEWMA-γ^2 charts. For example, in the case of $\gamma_0 = 0.05$, $\lambda = 0.2$, when the shift size $\tau = 1.1$ (see the 8th column in Table 1), the ATS_1 values of the VSI DEWMA1 $- \gamma^2$ chart, the VSI DEWMA2-γ^2 chart and the VSI DEWMA3-γ^2 chart are 23.4094, 27.6231 and 24.1732, respectively. By contrast, the ATS_1 values of the corresponding FSI DEWMA-γ^2 charts are 51.1236, 52.4819 and 53.8622, respectively. In addition, when the shift size is large, compared with the FSI DEWMA-γ^2 charts, the VSI DEWMA-γ^2 charts also have a remarkable improvement on the ATS performance. For example, considering the case of $\lambda = 0.2$ and $\tau = 2$ (see the last column in Table 1), the ATS_1 values of the VSI DEWMA-γ^2 charts are 0.4311, 0.7538 and 0.3094, respectively. These values are smaller compared with the ATS_1 values 3.3301, 3.3566 and 3.0361 of the corresponding FSI DEWMA-γ^2 charts. The same conclusion can be drawn when $ATS_0 = 500$ (see Table 5). These facts demonstrate the advantage of the VSI strategies applied to the FSI DEWMA-γ^2 charts.

Moreover, it is found that when the shift is large, a relatively large smoothing parameter is a better choice for the VSI DEWMA-γ^2 charts. If the shift size is small, a small smoothing parameter is generally suggested. For instance, in Table 1, when $\tau = 2$, the ATS_1 values of the VSI DEWMA1-γ^2 chart are 0.4718 for $\lambda = 0.1$, 0.4311 for $\lambda = 0.2$, 0.4254 for $\lambda = 0.25$, 0.4127 for $\lambda = 0.3$, 0.3924 for $\lambda = 0.5$, which indicates that the VSI DEWMA1-γ^2 chart with $\lambda = 0.5$ performs best for the detection of the shift $\tau = 2$ among the three VSI DEWMA1-γ^2 charts. These conclusions are applicable to the charts with other combinations of $(\gamma_0, \lambda, \tau)$ presented in Tables 2–4.

4.3. Performance comparison of the proposed VSI DEWMA-γ^2 charts and the existing VSI EWMA-γ^2 chart

Since the VSI EWMA-γ^2 chart has been proposed by Yeong et al. [1] to improve the EWMA-γ^2 chart's performance, it is interesting to compare the performances of the VSI EWMA-γ^2 chart and the proposed VSI DEWMA-γ^2 charts. To make a fair comparison, the parameter settings of n, γ_0, and λ of the VSI EWMA-γ^2 chart are the same as the ones of the VSI DEWMA-γ^2 charts in Section 4.1. We compute the out-of-control ATS_1 values of the VSI EWMA-γ^2 chart using the same procedure as for the VSI DEWMA-γ^2 charts. These results are also presented in Tables 1–4 for $ATS_0 = 370.4$ and in Table 5 for $ATS_0 = 500$.

Table 1. The out-of-control Average Time to Signal (ATS) (ATS_1), profiles of the Fixed Sampling Interval (FSI) and Variable Sampling Interval (VSI) charts for detecting increases when $n = 5$, $\gamma_0 = 0.05$, and $ATS_0 = 370.4$.

				τ										
λ		**W**	**K**	**1.00**	**1.05**	**1.08**	**1.10**	**1.12**	**1.15**	**1.18**	**1.20**	**1.25**	**1.50**	**2.00**
0.10	FSI EWMA	–	3.0711	370.1761	125.9979	75.9851	57.0914	44.3659	32.0632	24.2534	20.9079	15.0293	5.9765	2.7076
	VSI EWMA	0.3839	3.0711	367.1925	95.3155	49.0842	33.6479	24.0313	15.6478	10.9922	9.0893	6.1394	2.0920	0.7180
	FSI DEWMA1	–	1.9565	371.9701	99.8988	59.4064	45.3681	36.1028	27.4356	22.0509	19.5211	15.3436	8.0380	4.6153
	VSI DEWMA1	−0.1033	1.9565	373.9726	**57.5901**	**25.3622**	16.4788	11.3645	7.3350	5.1037	4.1395	2.8084	0.9609	0.4718
	FSI DEWMA2	–	2.0116	370.1005	102.6574	61.0207	46.5935	37.1306	28.0331	22.5166	19.9575	15.5966	8.1542	4.6910
	VSI DEWMA2	0.1257	2.0116	371.9510	67.1396	32.9105	23.0520	17.3331	12.4068	9.6902	8.4538	6.4700	2.9231	1.2464
	FSI DEWMA3	–	2.3486	369.9374	105.0872	62.3055	47.1234	37.4956	27.9354	22.2386	19.4885	14.9274	7.3356	4.0465
	VSI DEWMA3	−0.3660	2.3486	369.7578	60.0664	25.5217	**15.7505**	**10.5356**	**6.2406**	**4.1545**	**3.3106**	**2.1016**	**0.7528**	**0.4047**
0.20	FSI EWMA	–	3.4915	367.6269	144.7707	89.6274	68.3506	52.8366	37.7594	28.1110	23.7158	16.4010	5.7197	2.4737
	VSI EWMA	0.2864	3.4915	367.1162	116.8343	63.4213	44.3589	31.6098	20.1079	13.4960	10.7666	6.6229	1.7946	0.5821
	FSI DEWMA1	–	2.4561	371.9374	114.4798	68.2483	51.1265	39.4874	28.7839	22.1843	19.0867	14.0557	6.2401	3.3301
	VSI DEWMA1	−0.0936	2.4561	372.4466	**76.3116**	**35.9970**	**23.4094**	**15.9712**	9.8995	6.7465	5.4532	3.5442	1.0997	0.4311
	FSI DEWMA2	–	2.5087	372.4215	117.4660	69.9480	52.4819	40.7382	29.6186	22.6617	19.5552	14.3035	6.3084	3.3566
	VSI DEWMA2	0.1411	2.5087	374.2927	83.7125	41.2090	27.6231	19.5595	12.6818	8.9796	7.4912	5.2287	1.9566	0.7538
	FSI DEWMA3	–	3.1639	370.8202	120.1513	72.1159	53.8622	41.9704	30.3498	23.1330	19.7402	14.2842	5.9465	3.0361
	VSI DEWMA3	−0.3303	3.1639	369.5482	80.7134	37.8984	24.1732	16.3544	**9.7398**	**6.3007**	**4.8793**	**2.9434**	**0.7472**	**0.3094**
0.25	FSI EWMA	–	3.6406	369.1405	151.2074	95.7797	72.9416	56.6324	40.5410	30.3165	25.5196	17.4013	5.7622	2.4205
	VSI EWMA	0.2418	3.6406	368.8652	124.4290	69.7223	48.9792	35.1050	22.3901	15.1828	11.9823	7.1552	1.7351	0.5484
	FSI DEWMA1	–	2.6297	370.7037	121.0512	71.7788	53.5738	41.6461	30.0773	22.8707	19.5801	14.0884	5.8556	3.0105
	VSI DEWMA1	−0.0962	2.6297	371.1127	**84.4024**	**40.3410**	**26.3505**	**18.1208**	**11.1938**	**7.5119**	6.0232	3.8168	1.1363	0.4254
	FSI DEWMA2	–	2.6844	369.4576	123.1263	73.9222	55.4753	43.0381	30.7833	23.5396	20.0436	14.4415	5.9246	3.0346
	VSI DEWMA2	0.1342	2.6844	369.9462	90.4386	45.2194	30.4621	21.3549	13.4795	9.4201	7.6367	5.0744	1.7355	0.6564
	FSI DEWMA3	–	3.4750	371.1979	127.2163	77.2528	57.6786	44.6991	32.0639	24.0701	20.4424	14.6359	5.6594	2.7830
	VSI DEWMA3	−0.3167	3.4750	372.9638	90.4551	44.5125	28.8491	19.7339	11.8554	7.6387	**5.9696**	**3.5885**	**0.8680**	**0.3060**
0.30	FSI EWMA	–	3.7613	366.5147	155.9223	100.7280	76.6459	59.9813	43.2706	32.1587	26.8764	18.4106	5.8356	2.3908
	VSI EWMA	0.2057	3.7613	368.8578	130.9552	75.5753	53.2851	38.7282	25.0581	16.8371	13.2044	7.8627	1.7405	0.5254
	FSI DEWMA1	–	2.7887	371.9009	126.5173	75.9111	57.0042	44.1150	31.5882	23.8743	20.2318	14.3614	5.6331	2.7927
	VSI DEWMA1	−0.1007	2.7887	371.5815	**91.2559**	**44.7591**	**29.6942**	**20.4546**	**12.4966**	**8.3730**	**6.5902**	4.0980	1.1604	0.4127
	FSI DEWMA2	–	2.8418	369.8775	129.8109	78.5476	58.8517	45.4312	32.4678	24.4748	20.7149	14.7057	5.7015	2.8138
	VSI DEWMA2	0.1243	2.8418	370.2438	97.9086	49.9977	33.5739	23.5481	14.8185	10.0207	8.0327	5.1309	1.6116	0.5885
	FSI DEWMA3	–	3.7500	374.3353	132.7594	81.3221	60.7517	47.2190	33.8364	25.2441	21.3414	14.9772	5.4967	2.6106
	VSI DEWMA3	−0.3258	3.7500	374.7515	97.3536	49.0288	32.3040	22.1422	13.4342	8.6626	6.6660	**3.9143**	**0.8910**	**0.2949**
0.50	FSI EWMA	–	4.1245	375.6524	174.5985	115.5053	90.9618	72.2862	52.3737	39.4410	33.1150	22.4603	6.4264	2.3735
	VSI EWMA	0.0483	4.1245	376.0533	151.1212	91.2734	67.6243	50.5982	33.4621	23.0126	18.2747	10.7987	1.9183	0.4773
	FSI DEWMA1	–	3.3315	370.9195	145.4121	91.7765	69.7408	54.0177	38.8810	28.8153	24.0944	16.4516	5.4635	2.3571
	VSI DEWMA1	−0.1334	3.3315	368.3545	**114.0512**	**62.3124**	**43.0382**	**30.3708**	**19.1361**	**12.5449**	**9.7313**	**5.6516**	**1.2507**	**0.3924**
	FSI DEWMA2	–	3.3878	369.2664	148.1974	93.7432	71.2737	55.6849	39.6108	29.6477	24.8855	16.9849	5.5330	2.3835
	VSI DEWMA2	0.0635	3.3878	372.4184	121.7474	67.8213	47.4153	34.1365	21.5895	14.4472	11.3185	6.6779	1.4911	0.4725
	FSI DEWMA3	–	4.7500	370.3621	151.7613	96.1664	73.4374	57.1442	40.9715	30.4971	25.5357	17.3971	5.5028	2.2826
	VSI DEWMA3	−0.3820	4.7500	370.2821	121.6573	67.2042	46.8925	33.3385	21.0694	13.9586	10.8770	6.3655	1.4021	0.4326

Table 2. The out-of-control Average Time to Signal (ATS) (ATS_1), profiles of the Fixed Sampling Interval (FSI) and Variable Sampling Interval (VSI) charts for detecting increases when $n = 5$, $\gamma_0 = 0.1$, and $ATS_0 = 370.4$.

				τ										
λ		**W**	**K**	**1.00**	**1.05**	**1.08**	**1.10**	**1.12**	**1.15**	**1.18**	**1.20**	**1.25**	**1.50**	**2.00**
0.10	FSI EWMA	–	3.1166	367.6124	125.9636	76.1815	57.1776	44.5906	32.0879	24.5879	20.9279	15.1918	6.0345	2.7433
	VSI EWMA	0.4139	3.1166	368.1795	96.2092	49.7179	33.9645	24.3198	15.8338	11.2523	9.2254	6.2975	2.1702	0.7575
	FSI DEWMA1	–	2.0354	370.6626	101.2174	60.4328	45.9322	36.8447	28.1069	22.6350	19.9092	15.6259	8.1993	4.7147
	VSI DEWMA1	−0.0469	2.0354	369.0254	**59.1033**	26.9575	17.6812	12.7345	8.4203	6.1168	5.1154	3.4683	1.2254	0.5389
	FSI DEWMA2	–	2.0825	368.4446	102.8437	61.8386	47.1830	37.5096	28.4423	23.0225	20.2849	15.8906	8.3113	4.7764
	VSI DEWMA2	0.1562	2.0825	366.7810	66.8060	33.5772	23.6522	17.8497	12.9994	10.2999	9.0274	6.9658	3.2688	1.4281
	FSI DEWMA3	–	2.4174	371.6181	106.0751	62.8333	47.4767	37.6269	28.0659	22.2268	19.5025	14.9643	7.3352	4.0453
	VSI DEWMA3	−0.3291	2.4174	370.7066	60.2679	**25.4360**	**15.6782**	**10.4000**	**6.1823**	**4.0465**	**3.2199**	**2.0337**	**0.7495**	**0.4045**
0.20	FSI EWMA	–	3.5360	367.7989	143.5643	89.9943	68.7605	53.0518	38.1029	28.3589	23.8811	16.6600	5.7652	2.5027
	VSI EWMA	0.3039	3.5360	367.9264	116.0666	63.6802	44.5902	31.7007	20.2839	13.6466	10.8776	6.7184	1.8201	0.5962
	FSI DEWMA1	–	2.5122	368.4945	116.1500	68.6111	51.2835	39.9319	29.0339	22.5136	19.2856	14.2614	6.3173	3.3628
	VSI DEWMA1	−0.0475	2.5122	368.2580	**77.9104**	**36.6848**	**23.9138**	**16.4909**	10.4676	7.2205	5.8671	3.9228	1.2813	0.4905
	FSI DEWMA2	–	2.5613	371.2616	118.2724	70.3846	52.5748	41.1312	29.7562	23.0080	19.7130	14.4925	6.3766	3.3997
	VSI DEWMA2	0.1601	2.5613	369.3221	83.4470	40.9072	27.4224	19.6684	12.7359	9.2024	7.6184	5.3466	2.0388	0.7993
	FSI DEWMA3	–	3.2264	368.0910	120.5823	72.5441	54.3478	42.2450	30.5696	23.3444	19.9857	14.3629	5.9782	3.0490
	VSI DEWMA3	−0.2887	3.2264	369.8869	82.1467	38.6326	24.8593	16.7192	**9.9286**	**6.4324**	**5.0049**	**2.9514**	**0.7483**	**0.3120**
0.25	FSI EWMA	–	3.6906	370.2542	152.1340	96.6275	73.4577	57.6143	41.1211	30.7453	25.7566	17.6357	5.8337	2.4535
	VSI EWMA	0.2595	3.6906	371.1780	125.4023	70.4269	49.3873	35.8201	22.8631	15.4196	12.1254	7.3132	1.7775	0.5622
	FSI DEWMA1	–	2.6867	371.1888	121.1996	73.0623	54.4689	42.3414	30.5373	23.3042	19.7989	14.2879	5.9290	3.0372
	VSI DEWMA1	−0.0485	2.6867	372.8129	**85.1426**	**41.4990**	**27.3367**	**18.8783**	11.7496	7.9784	6.3770	4.1088	1.2767	0.4712
	FSI DEWMA2	–	2.7336	370.0864	123.7209	74.6037	56.1182	43.2382	31.1729	23.7447	20.2243	14.5673	5.9937	3.0721
	VSI DEWMA2	0.1538	2.7336	368.5892	90.3392	45.3162	30.5953	21.3902	13.6772	9.5229	7.7549	5.1658	1.8082	0.6833
	FSI DEWMA3	–	3.5375	369.8128	127.7132	77.4857	57.8641	44.7633	32.3323	24.2914	20.8569	14.7437	5.7012	2.8067
	VSI DEWMA3	−0.3140	3.5375	366.7154	89.3815	43.7066	28.4360	19.3158	**11.6628**	**7.5213**	**5.9254**	**3.5116**	**0.8419**	**0.3063**
0.30	FSI EWMA	–	3.8177	371.5150	157.9810	101.2323	78.4343	61.1664	44.0347	32.7301	27.3322	18.6694	5.9467	2.4187
	VSI EWMA	0.2088	3.8177	370.2695	131.1985	74.9908	53.8761	38.9647	25.1284	16.8936	13.2471	7.8513	1.7662	0.5291
	FSI DEWMA1	–	2.8398	370.2776	127.5789	77.0256	57.7853	44.5458	32.0361	24.1558	20.4117	14.6005	5.7014	2.8201
	VSI DEWMA1	−0.0673	2.8398	368.7707	**91.8084**	**45.5975**	**30.2380**	**20.7502**	**12.8422**	**8.5294**	6.7648	4.2369	1.2381	0.4451
	FSI DEWMA2	–	2.8898	368.4789	129.9920	78.8621	58.9230	45.4257	32.7215	24.6721	20.9896	14.9249	5.7613	2.8425
	VSI DEWMA2	0.1445	2.8898	367.4216	97.8038	50.0258	33.6596	23.4654	14.9823	10.1835	8.1632	5.2587	1.6620	0.6100
	FSI DEWMA3	–	3.8156	370.6379	133.2351	81.2088	61.2992	47.3695	34.1142	25.3709	21.5414	15.1259	5.5529	2.6276
	VSI DEWMA3	−0.3018	3.8156	371.9241	97.8854	49.0931	32.6608	22.3693	13.6071	8.6902	**6.7356**	**3.9586**	**0.8862**	**0.2973**
0.50	FSI EWMA	–	4.1777	370.5010	172.9758	116.6594	90.7307	72.4252	52.8353	39.7950	33.5760	22.7229	6.5079	2.4068
	VSI EWMA	0.0653	4.1777	372.4327	150.3717	92.6034	67.7999	50.9389	33.8943	23.3695	18.5897	10.9711	1.9703	0.4900
	FSI DEWMA1	–	3.3813	371.7854	147.5367	92.2987	70.3034	54.5683	39.0332	29.0453	24.4393	16.8330	5.5217	2.3858
	VSI DEWMA1	−0.0973	3.3813	371.7138	**116.9647**	**63.3311**	**43.9179**	**31.1024**	**19.5326**	**12.8722**	**10.0616**	**5.9160**	**1.2933**	**0.4102**
	FSI DEWMA2	–	3.4375	370.7572	149.9639	94.6078	72.3029	56.2172	40.2634	29.9471	25.1701	17.2605	5.6377	2.4144
	VSI DEWMA2	0.0645	3.4375	368.4288	121.0762	67.2412	47.3187	33.8055	21.4994	14.3077	11.2384	6.6687	1.5029	0.4738
	FSI DEWMA3	–	4.8188	368.7266	151.4076	96.7950	73.7670	57.5661	41.3584	30.7512	25.7550	17.5012	5.5765	2.3200
	VSI DEWMA3	−0.3557	4.8188	372.0568	122.7536	68.4165	47.5859	34.0744	21.5377	14.2606	11.0801	6.4822	1.4235	0.4472

Table 3. The out-of-control Average Time to Signal (ATS) (ATS_1), profiles of the Fixed Sampling Interval (FSI) and Variable Sampling Interval (VSI) charts for detecting increases when $n = 5$, $\gamma_0 = 0.15$, and $ATS_0 = 370.4$.

				τ										
λ		W	K	1.00	1.05	1.08	1.10	1.12	1.15	1.18	1.20	1.25	1.50	2.00
0.10	FSI EWMA	–	3.1984	369.0763	126.1550	76.5635	57.7625	45.0043	32.5398	24.8350	21.4311	15.5086	6.1376	2.8002
	VSI EWMA	0.4498	3.1984	369.6664	95.8789	49.7076	34.1828	24.5588	16.0583	11.4734	9.5499	6.5141	2.2754	0.8054
	FSI DEWMA1	–	2.1604	371.3643	102.3826	61.3798	47.0794	37.6496	28.7759	23.1580	20.5391	16.1523	8.4631	4.8480
	VSI DEWMA1	0.0680	2.1604	372.0128	63.1585	30.7392	21.5400	16.1356	11.6024	8.9243	7.7395	5.8271	2.4621	1.0253
	FSI DEWMA2	–	2.2038	371.0508	105.1677	62.6169	48.2412	38.5494	29.3190	23.5536	20.8224	16.3350	8.5535	4.8913
	VSI DEWMA2	0.2342	2.2038	372.3204	69.9651	35.3425	25.3639	19.6055	14.5394	11.6526	10.3602	8.1399	3.9953	1.8410
	FSI DEWMA3	–	2.5258	367.8827	105.5097	63.1666	47.4851	37.6491	28.1878	22.2422	19.5804	14.9980	7.3070	4.0063
	VSI DEWMA3	−0.2546	2.5258	368.3701	**60.1293**	**25.7724**	**15.6249**	**10.2902**	**6.0682**	**3.9318**	**3.1473**	**2.0047**	**0.7440**	**0.4006**
0.20	FSI EWMA	–	3.6221	369.7990	145.4220	91.6824	69.9146	54.0355	38.7932	29.0184	24.5336	17.0218	5.9419	2.5599
	VSI EWMA	0.3396	3.6221	372.8690	118.2961	65.3854	45.6393	32.5418	20.7928	14.0832	11.2415	6.9578	1.9071	0.6355
	FSI DEWMA1	–	2.6091	371.9232	116.4975	69.6164	52.2476	40.7988	29.8254	22.9290	19.6802	14.5618	6.4562	3.4368
	VSI DEWMA1	0.0321	2.6091	372.2021	**78.9243**	**38.0889**	**25.2155**	17.6640	11.4589	8.0863	6.6579	4.5711	1.6164	0.6142
	FSI DEWMA2	–	2.6526	370.1323	119.4287	71.4717	53.5234	41.7415	30.3033	23.2862	20.1378	14.8237	6.5166	3.4545
	VSI DEWMA2	0.2155	2.6526	370.7427	85.1893	42.4286	28.5717	20.3250	13.4664	9.7138	8.2007	5.7953	2.3047	0.9156
	FSI DEWMA3	–	3.3389	370.2726	123.0005	73.6284	55.3222	42.9047	31.0046	23.7215	20.1796	14.5848	6.0366	3.0713
	VSI DEWMA3	−0.2434	3.3389	372.5822	83.7440	39.3817	25.2904	**16.9293**	**10.0395**	**6.5189**	**5.0256**	**2.9604**	**0.7483**	**0.3126**
0.25	FSI EWMA	—-	3.7734	369.1385	152.9961	97.5683	74.8285	58.3224	42.0705	31.2092	26.2280	17.9885	5.9670	2.5113
	VSI EWMA	0.2801	3.7734	369.0245	125.4836	70.7344	50.0679	36.0386	23.1990	15.5410	12.2788	7.4215	1.8237	0.5850
	FSI DEWMA1	–	2.7770	369.6915	123.3540	73.6058	55.5396	43.0745	31.1510	23.7612	20.2131	14.6253	6.0700	3.0992
	VSI DEWMA1	0.0180	2.7770	370.5275	**87.0394**	**42.4098**	**28.1878**	**19.6348**	12.4441	8.5378	6.8857	4.5241	1.4721	0.5471
	FSI DEWMA2	–	2.8270	373.7214	126.2723	76.2099	57.2167	44.3580	32.0348	24.2784	20.7941	15.0020	6.1269	3.1254
	VSI DEWMA2	0.1944	2.8270	370.9195	91.7741	46.2695	31.3164	22.0770	14.1940	9.8887	8.1326	5.4812	1.9575	0.7565
	FSI DEWMA3	–	3.6438	368.9060	129.1135	78.4511	58.7081	45.5555	32.5492	24.8947	20.9758	14.8963	5.7911	2.8208
	VSI DEWMA3	−0.2678	3.6438	368.0103	91.1904	44.7378	29.1266	19.8130	**11.8344**	**7.7727**	**5.9775**	**3.5314**	**0.8529**	**0.3070**
0.30	FSI EWMA	–	3.9048	370.7528	159.1213	102.5530	79.1717	62.3167	44.6769	33.3432	27.9511	19.0375	6.0698	2.4861
	VSI EWMA	0.2440	3.9048	373.6455	133.6288	76.7927	55.0278	40.1690	25.8428	17.4374	13.7432	8.1390	1.8358	0.5588
	FSI DEWMA1	–	2.9271	370.8609	129.0580	77.9693	58.7668	45.4089	32.6721	24.6964	20.9058	14.9406	5.8337	2.8654
	VSI DEWMA1	0.0003	2.9271	370.7731	**93.7161**	**46.7735**	**31.2911**	**21.6727**	**13.5232**	9.1040	7.2709	4.6455	1.3971	0.5008
	FSI DEWMA2	–	2.9740	370.3527	131.8398	79.9923	60.1329	46.5962	33.4245	25.2433	21.5565	15.1912	5.8733	2.8996
	VSI DEWMA2	0.1859	2.9740	370.1649	99.4660	51.0634	34.5354	24.3149	15.4400	10.5753	8.5272	5.5021	1.7832	0.6704
	FSI DEWMA3	–	3.9250	370.9439	134.0905	82.3402	62.3112	48.3538	34.6312	25.9411	21.9530	15.3622	5.6430	2.6629
	VSI DEWMA3	−0.2754	3.9250	371.0242	98.3427	49.6918	33.1808	22.7811	13.7089	**8.8509**	**6.8246**	**3.9800**	**0.8964**	**0.3010**
0.50	FSI EWMA	–	4.2748	370.1304	173.8552	117.6483	92.3405	73.8995	53.9268	40.7369	34.1582	23.2073	6.6981	2.4660
	VSI EWMA	0.0835	4.2748	371.5374	150.9331	93.3622	68.9214	51.9348	34.5886	23.8904	18.9058	11.1896	2.0229	0.5044
	FSI DEWMA1	–	3.4637	371.1363	147.7779	93.8732	71.8223	55.9494	39.8960	29.8366	25.0625	17.2310	5.6468	2.4413
	VSI DEWMA1	−0.0585	3.4637	370.0119	**116.9489**	**64.4807**	**44.9605**	**31.9572**	**19.9815**	**13.2923**	**10.3709**	6.0926	1.3644	0.4335
	FSI DEWMA2	–	3.5199	373.0158	151.3238	96.2231	73.5083	57.6697	41.2336	30.8517	25.8476	17.6476	5.7602	2.4667
	VSI DEWMA2	0.1100	3.5199	375.6547	124.3593	69.6053	48.9131	35.3430	22.4818	15.0869	11.8507	6.9816	1.5822	0.5079
	FSI DEWMA3	–	4.9453	368.6626	152.6639	97.8498	74.9566	58.6310	42.2095	31.4035	26.3804	17.9053	5.6952	2.3675
	VSI DEWMA3	−0.3517	4.9453	367.0269	121.4532	67.5080	46.9180	33.4541	20.9453	13.6444	10.5264	**5.9041**	**1.0269**	**0.2843**

Table 4. The out-of-control Average Time to Signal (ATS) (ATS_1), profiles of the Fixed Sampling Interval (FSI) and Variable Sampling Interval (VSI) charts for detecting increases when $n = 5$, $\gamma_0 = 0.20$, and $ATS_0 = 370.4$.

				τ										
λ		W	K	**1.00**	**1.05**	**1.08**	**1.10**	**1.12**	**1.15**	**1.18**	**1.20**	**1.25**	**1.50**	**2.00**
0.10	FSI EWMA	–	3.3194	372.3208	128.1366	78.1298	58.9182	45.8026	33.3928	25.6028	21.8990	15.9114	6.3531	2.8825
	VSI EWMA	0.4927	3.3194	370.1783	96.1321	49.9762	34.2837	24.6219	16.2640	11.7555	9.6637	6.6725	2.4180	0.8731
	FSI DEWMA1	–	2.3374	372.3872	105.0884	63.5560	48.8266	39.0044	29.8071	24.1654	21.4403	16.7756	8.7991	5.0117
	VSI DEWMA1	0.2235	2.3374	374.3406	68.0586	35.0681	25.2254	19.4912	14.6271	11.8000	10.4909	8.2235	4.0079	1.8460
	FSI DEWMA2	–	2.3702	372.1632	106.2442	64.2080	49.3349	39.5792	30.0978	24.3436	21.5295	16.9579	8.8666	5.0429
	VSI DEWMA2	0.3407	2.3702	372.4202	71.4070	37.5893	27.3714	21.4493	16.1937	13.2268	11.8279	9.4548	4.8706	2.3560
	FSI DEWMA3	–	2.6801	367.5595	106.5234	63.4544	48.1225	38.3160	28.4493	22.4445	19.6392	15.0387	7.3007	3.9860
	VSI DEWMA3	−0.1740	2.6801	364.6602	**60.2111**	**25.2506**	**15.5223**	**10.0854**	**5.8555**	**3.8112**	**3.0137**	**1.9375**	**0.7405**	**0.3986**
0.20	FSI EWMA	–	3.7425	371.1968	148.4859	93.4543	71.2538	55.5064	39.7373	29.8807	25.2655	17.4849	6.1178	2.6513
	VSI EWMA	0.3655	3.7425	370.8363	119.2478	65.4883	45.8219	32.7490	20.8839	14.2156	11.4524	7.0724	1.9596	0.6745
	FSI DEWMA1	–	2.7403	368.4572	117.9049	70.8812	53.4586	41.8790	30.5285	23.6317	20.3610	15.0599	6.6560	3.5174
	VSI DEWMA1	0.1333	2.7403	366.9848	**80.6926**	**39.5883**	26.7328	19.0965	12.5996	9.1316	7.6207	5.4048	2.0516	0.8073
	FSI DEWMA2	–	2.7819	369.7447	121.6273	72.6772	54.7748	43.0087	31.1197	24.0975	20.7060	15.2149	6.6945	3.5365
	VSI DEWMA2	0.2782	2.7819	367.5243	86.1142	42.8720	29.2762	21.2786	14.1261	10.3304	8.7678	6.2427	2.6027	1.0665
	FSI DEWMA3	–	3.4932	371.7855	123.8824	75.0594	56.6154	43.8229	31.7715	24.2908	20.6244	14.8716	6.1271	3.1052
	VSI DEWMA3	−0.1942	3.4932	371.5118	83.7239	39.7021	**25.5851**	**17.1193**	**10.1613**	**6.5077**	**5.0332**	**2.9301**	**0.7444**	**0.3161**
0.25	FSI EWMA	–	3.8975	367.8178	154.5534	99.5409	75.9644	59.8661	42.8120	32.2125	27.0839	18.6109	6.1630	2.5953
	VSI EWMA	0.3045	3.8975	364.8145	125.4269	71.3575	50.1242	36.4595	23.2885	15.8038	12.4727	7.5524	1.8978	0.6206
	FSI DEWMA1	–	2.9043	372.9700	125.2344	75.7097	56.8647	44.1461	32.1109	24.4162	20.9148	15.0596	6.2168	3.1855
	VSI DEWMA1	0.1211	2.9043	376.1036	**90.0527**	**44.7549**	30.0313	21.0002	13.6143	9.4998	7.7465	5.2182	1.8177	0.6948
	FSI DEWMA2	–	2.9415	369.5504	127.2032	77.0285	57.9755	44.9788	32.5979	24.9564	21.2697	15.2902	6.2923	3.2060
	VSI DEWMA2	0.2574	2.9415	367.7000	92.8604	47.2572	31.9915	22.7370	14.8439	10.5180	8.6448	5.8688	2.2057	0.8701
	FSI DEWMA3	–	3.8031	370.5651	131.2566	80.0270	60.2550	46.5168	33.4969	25.3841	21.4223	15.2345	5.8799	2.8707
	VSI DEWMA3	−0.2173	3.8031	368.8953	92.4869	45.1942	**29.5266**	**19.9287**	**11.8288**	**7.5769**	**5.7957**	**3.3263**	**0.7627**	**0.2966**
0.30	FSI EWMA	–	4.0336	371.3933	160.4681	105.2128	80.9225	63.2229	46.0355	34.5588	28.9034	19.6627	6.2809	2.5639
	VSI EWMA	0.2679	4.0336	372.1265	133.7468	78.0956	55.6440	40.2904	26.3108	17.8143	13.9840	8.3013	1.9009	0.5923
	FSI DEWMA1	–	3.0480	371.1150	130.1812	80.0030	60.0115	46.6943	33.6600	25.4425	21.6556	15.3478	5.9833	2.9404
	VSI DEWMA1	0.0733	3.0480	367.9363	**93.9890**	**48.1327**	**32.1844**	**22.5033**	14.2340	9.6599	7.7588	4.9882	1.5930	0.5875
	FSI DEWMA2	–	3.0887	369.0223	132.8219	81.3847	61.6387	47.5806	34.4358	26.0090	21.9558	15.6014	6.0230	2.9554
	VSI DEWMA2	0.2510	3.0887	372.2057	101.3577	52.6550	36.0397	25.3255	16.3154	11.1881	9.0666	5.9003	1.9926	0.7602
	FSI DEWMA3	–	4.0875	369.8800	137.5264	84.2052	63.6060	49.3653	35.4756	26.6924	22.5659	15.7882	5.7721	2.7064
	VSI DEWMA3	−0.2456	4.0875	366.8376	99.9052	50.3313	33.5086	22.9453	**13.8713**	**8.9721**	**6.8912**	**4.0180**	**0.8913**	**0.3034**
0.50	FSI EWMA	–	4.4255	370.8789	177.3040	120.1001	94.5725	75.4207	55.4303	42.2820	35.4128	24.2024	6.9641	2.5758
	VSI EWMA	0.1037	4.4255	370.4141	153.0493	94.6782	70.1921	52.6492	35.3184	24.6357	19.4645	11.6010	2.0869	0.5377
	FSI DEWMA1	–	3.5875	371.8886	150.7094	96.5457	73.1837	57.6905	41.2434	30.8084	26.1479	17.8784	5.8772	2.5238
	VSI DEWMA1	0.0016	3.5875	371.8905	**119.9841**	**66.8757**	**46.2760**	**33.4296**	**20.8960**	**13.9637**	11.0195	6.4788	1.4777	0.4768
	FSI DEWMA2	–	3.6344	370.5396	153.2701	98.0307	75.0025	58.6100	42.0502	31.5994	26.5117	18.2001	5.9388	2.5440
	VSI DEWMA2	0.1363	3.6344	368.7202	124.2083	69.9987	49.2641	35.4423	22.6400	15.2415	11.9794	7.1492	1.6485	0.5403
	FSI DEWMA3	–	5.1375	370.7534	155.0373	99.8718	76.8015	60.3359	43.3409	32.4687	27.2780	18.6121	5.8794	2.4376
	VSI DEWMA3	−0.3203	5.1375	369.3511	123.7867	69.2212	48.3863	34.6306	21.6426	14.2060	**10.9812**	**6.1759**	**1.0748**	**0.2929**

Table 5. The out-of-control Average Time to Signal (ATS) (ATS_1), profiles of the Fixed Sampling Interval (FSI) and Variable Sampling Interval (VSI) charts for detecting increases when $n = 5$, $\gamma_0 = 0.05$, and $ATS_0 = 500$.

λ		W	K	τ = 1.00	1.05	1.08	1.10	1.12	1.15	1.18	1.20	1.25	1.50	2.00
0.10	FSI EWMA	–	3.2388	500.3701	158.2376	91.6049	67.0707	51.3721	36.3179	27.2957	23.1459	16.4301	6.2919	2.8149
	VSI EWMA	0.4063	3.2388	503.0998	120.1558	58.8344	38.9590	27.2396	17.2927	11.9621	9.7503	6.4931	2.1693	0.7447
	FSI DEWMA1	–	2.1390	497.5862	121.7953	69.6163	52.0624	40.9642	30.4380	24.1344	21.3160	16.5113	8.5098	4.8625
	VSI DEWMA1	−0.0950	2.1390	495.3687	**67.9458**	**28.4750**	17.9626	12.2781	7.8206	5.4613	4.5138	2.9937	1.0237	0.4993
	FSI DEWMA2	–	2.1922	501.6439	125.5753	71.9934	53.5035	41.8420	31.1764	24.7806	21.7166	16.7443	8.6241	4.9245
	VSI DEWMA2	0.1375	2.1922	502.3128	79.3788	36.9943	25.0687	18.4700	13.1398	10.2247	8.9132	6.7734	3.0986	1.3320
	FSI DEWMA3	–	2.6081	501.5279	129.4471	73.8147	54.7295	42.4515	31.3830	24.5841	21.3626	16.2070	7.7963	4.2733
	VSI DEWMA3	−0.3500	2.6081	499.1221	72.6740	29.3045	**17.6404**	**11.5362**	**6.8152**	**4.4751**	**3.5447**	**2.2401**	**0.8025**	**0.4274**
0.20	FSI EWMA	–	3.6725	498.2100	184.2453	111.3474	83.3029	63.6105	44.3628	32.5121	27.1105	18.3649	6.0765	2.5585
	VSI EWMA	0.2875	3.6725	495.7551	147.2292	77.6077	52.9951	37.0178	22.8589	15.0442	11.8258	7.0606	1.8200	0.5883
	FSI DEWMA1	–	2.6288	499.8257	142.7494	81.7266	59.8030	46.0732	32.6374	24.7908	21.1572	15.2569	6.5528	3.4535
	VSI DEWMA1	−0.0800	2.6288	501.5546	**94.1346**	**42.2327**	**26.6899**	**18.0486**	10.9275	7.3778	5.9230	3.7929	1.1837	0.4556
	FSI DEWMA2	–	2.6788	500.9586	147.3096	84.0863	61.8827	47.1779	33.5023	25.4131	21.5893	15.5974	6.6250	3.4910
	VSI DEWMA2	0.1500	2.6788	503.6521	103.5149	48.2802	31.5372	21.7273	13.8125	9.6947	7.9468	5.4607	2.0229	0.7868
	FSI DEWMA3	–	3.4326	499.9738	151.6689	87.0950	64.6513	49.1668	34.7180	25.9634	22.0500	15.6533	6.2962	3.1733
	VSI DEWMA3	−0.3050	3.4326	501.0199	101.5828	45.5354	28.7177	18.8703	**10.9014**	**6.8982**	**5.3868**	**3.1625**	**0.7938**	**0.3242**
0.25	FSI EWMA	–	3.8275	500.5327	194.0071	119.7949	89.9373	68.7134	48.1205	35.3406	29.2768	19.5993	6.1370	2.5176
	VSI EWMA	0.2388	3.8275	497.3182	157.8102	85.8077	59.1564	41.7027	25.9254	17.0927	13.2423	7.7166	1.7700	0.5562
	FSI DEWMA1	–	2.8100	503.0799	151.9037	87.6480	64.5135	48.9813	34.6154	25.7883	21.9114	15.5031	6.1566	3.1277
	VSI DEWMA1	−0.0950	2.8100	499.9888	**103.8500**	**47.8499**	**30.5780**	**20.4271**	**12.2419**	**8.0722**	6.3955	4.0084	1.1750	0.4364
	FSI DEWMA2	–	2.8563	498.9085	155.6457	90.4400	66.0824	50.4546	35.5338	26.4844	22.3478	15.8314	6.2461	3.1538
	VSI DEWMA2	0.1400	2.8563	499.6960	112.9963	54.2746	35.3120	24.2547	15.0078	10.1304	8.1724	5.3095	1.7957	0.6776
	FSI DEWMA3	–	3.7381	494.0873	160.1013	93.6017	68.7743	52.1968	36.8809	27.3430	23.0753	16.0080	6.0097	2.8988
	VSI DEWMA3	−0.3200	3.7381	491.6257	111.5303	52.2414	33.3195	22.0989	13.0417	8.2912	**6.3821**	**3.7501**	**0.8952**	**0.3167**
0.30	FSI EWMA	–	3.9606	502.1732	201.6890	126.8471	96.1862	73.9827	51.9160	37.9639	31.6967	20.9850	6.2535	2.4798
	VSI EWMA	0.1988	3.9606	500.7416	167.0539	93.5837	65.4970	46.6089	29.1815	19.1634	15.0162	8.6008	1.7750	0.5290
	FSI DEWMA1	–	2.9650	498.0808	159.9758	93.0829	68.4371	52.2216	36.5454	26.9979	22.8141	15.8718	5.9439	2.8864
	VSI DEWMA1	−0.0900	2.9650	499.0090	**114.7532**	**54.4348**	**35.1379**	**23.7287**	**14.1287**	**9.1752**	**7.2062**	4.3749	1.2120	0.4290
	FSI DEWMA2	–	3.0167	501.0662	164.5357	96.1804	70.6732	53.7758	37.7176	27.7275	23.4370	16.1895	6.0168	2.9135
	VSI DEWMA2	0.1250	3.0167	498.7375	122.1366	59.8475	39.2680	26.9229	16.4366	10.8663	8.6901	5.3615	1.6448	0.5966
	FSI DEWMA3	–	4.0225	493.8551	168.7798	99.5118	73.9771	55.8016	39.0334	28.8901	24.1397	16.5876	5.8469	2.7129
	VSI DEWMA3	−0.3100	4.0225	496.3372	123.5366	59.6243	38.8380	25.7896	15.1408	9.6456	7.4245	**4.2158**	**0.9354**	**0.3068**
0.50	FSI EWMA	–	4.3359	500.2254	224.9025	147.6832	113.6327	89.8891	64.0376	47.4220	39.3385	26.0574	7.0357	2.4694
	VSI EWMA	0.0588	4.3359	504.0409	195.9529	117.4152	84.8916	63.0491	40.9502	27.6460	21.6219	12.4303	2.0533	0.4895
	FSI DEWMA1	–	3.5213	503.4475	187.6644	114.6368	86.0171	65.7948	46.0245	33.6178	27.9151	18.7848	5.8217	2.4530
	VSI DEWMA1	−0.1200	3.5213	503.3256	**148.1737**	**78.0700**	**53.1243**	**36.8910**	**22.5014**	**14.5221**	**11.1032**	**6.3541**	**1.3076**	**0.4067**
	FSI DEWMA2	–	3.5753	501.9253	190.5824	117.2167	88.3294	67.5367	47.4165	34.6380	28.8163	19.2969	5.9226	2.4648
	VSI DEWMA2	0.0500	3.5753	499.1394	153.3876	82.7559	57.1241	40.1449	24.8961	16.2248	12.6066	7.2511	1.5160	0.4722
	FSI DEWMA3	–	5.0525	498.5600	193.0825	120.1521	90.3966	69.4843	48.5561	35.7812	29.6747	19.7589	5.8934	2.3801
	VSI DEWMA3	−0.3750	5.0525	498.9624	154.3364	83.5859	57.1709	40.0364	24.5905	16.0325	12.3243	6.9906	1.4569	0.4503

It is observed from these tables that the VSI DEWMA1-γ^2 chart and the VSI DEWMA3-γ^2 chart generally perform better than the VSI EWMA-γ^2 chart regardless of the value of the shift. For instance, when there is a small shift, such as $\tau = 1.05$, with $\gamma_0 = 0.1$, $\lambda = 0.2$ (see Table 2), the ATS_1 values of the VSI DEWMA1-γ^2 chart and the VSI DEWMA3-γ^2 chart are 77.9104 and 82.1647, respectively. Both values are smaller than the $ATS_1 = 116.0666$ of the VSI EWMA $- \gamma^2$ chart. When there is a large shift, such as $\tau = 2$, the ATS_1 values of these three charts are 0.4905, 0.3120 and 0.5962, respectively.

Moreover, the VSI DEWMA2-γ^2 chart has a better performance than the VSI EWMA-γ^2 chart when the shift is small to moderate ($1 < \tau \leq 1.2$). When the shift is large, the VSI EWMA-γ^2 chart is superior to the VSI DEWMA2-γ^2 chart. For example, when $\tau = 1.05$, $\gamma_0 = 0.1$ and $\lambda = 0.2$, the $ATS_1 = 83.4470$ of the VSI DEWMA2-γ^2 chart is smaller than $ATS_1 = 116.0666$ of the VSI EWMA-γ^2 chart. When the shift size increases up to $\tau = 2$, the $ATS_1 = 0.7993$ of the VSI DEWMA2-γ^2 chart is larger than ATS_1=0.5962 of the VSI EWMA-γ^2 chart.

In addition, it is worth noting that the VSI strategy has a greater influence on the performance of the DEWMA charts than on the EWMA chart in most cases. Considering the example described above (λ=0.2 in Table 2), the ATS_1 of the FSI EWMA-γ^2 chart, the FSI DEWMA1-γ^2 chart, the FSI DEWMA2-γ^2 chart and the FSI DEWMA3- γ^2 chart are 143.5643, 116.1500, 118.2724, 120.5823 for τ= 1.05 and 2.5027, 3.3628, 3.3997, 3.0490 for τ= 2. The ATS_1 for the VSI EWMA-γ^2 chart, the VSI DEWMA1-γ^2 chart, the VSI DEWMA2-γ^2 chart and the VSI DEWMA3-γ^2 chart are 116.0666, 77.9104, 83.7740, 82.1467 for τ = 1.05 and 0.5962, 0.4905, 0.7993, 0.3120 for τ=2. The reduced ATS values, which are defined as ATS_1^R= $ATS_1^{FSI} - ATS_1^{VSI}$, of these charts due to the application of the VSI strategies are 27.4977, 38.2395, 34.8253 and 38.4356 for $\tau = 1.05$ and 1.9066, 2.8724, 2.6004, 2.7371 for $\tau = 2$. Obviously, compared with the VSI EWMA-γ^2 chart, implementation of VSI strategies to the DEWMA CV charts reduces the time to trigger a signal when the process is out-of-control. These findings can also be verified based on the results in other cases as shown in Tables 1–4.

4.4. Comparison among the proposed three VSI DEWMA-γ^2 charts

Sections 4.2 and 4.3 have compared the performance of the proposed VSI DEWMA-γ^2 charts with other charts. In this subsection, we compare the ATS_1 performances among the proposed VSI DEWMA-γ^2 charts.

From Tables 1–4, we can see that the VSI DEWMA1-γ^2 chart and the VSI DEWMA3-γ^2 chart always perform better than the VSI DEWMA2-γ^2 chart under different shifts regardless of the values of λ and γ_0. For example, when $\gamma_0 = 0.1$ and $\lambda = 0.25$ (see Table 2), the VSI DEWMA1-γ^2 chart yields the smallest among three charts for $1.05 \leq \tau \leq 1.12$, and the VSI DEWMA3-γ^2 chart yields the smallest ATS_1 among three charts for $1.15 \leq \tau \leq 2$. On the other hand, the VSI DEWMA2-γ^2 chart always yields the largest ATS_1 among three charts, regardless of the shift size.

The advantage of the VSI DEWMA3-γ^2 chart over the VSI DEWMA1- γ^2 chart is generally significant when the value of λ is small. The VSI DEWMA1-γ^2 chart's performance becomes much better than the VSI DEWMA3-γ^2 chart when λ increases. For instance, in Table 1, when $\lambda = 0.1$, the VSI DEWMA3-γ^2 chart performs better than the VSI DEWMA1-γ^2 chart for the shift range $1.08 \leq \tau \leq 2$. If λ increases up to 0.5, the VSI DEWMA1-γ^2 chart performs better than the VSI DEWMA3-γ^2 chart for all shifts.

In addition, for a fixed value of λ, with the increase in γ_0, the range in which the VSI DEWMA3-γ^2 chart performs better than the VSI DEWMA1-γ^2 chart becomes wider. For instance, when $\gamma = 0.1$, with the increase in γ_0, say γ_0 increases from 0.05 (Table 1) up to 0.2 (Table 4), the range in which the VSI DEWMA3-γ^2 chart performs better than the VSI DEWMA1-γ^2 chart widens from $1.12 \leq \tau \leq 2$ to $1.05 \leq \tau \leq 2$. Also, with the increase in γ_0, the out-of-control ATS_1 values of the VSI DEWMA1-γ^2 chart and the DEWMA2-γ^2 chart have an increasing trend. For instance, for the shift size $\tau = 1.05$ and $\lambda = 0.1$, if γ_0 increases from 0.05 (see Table 1) up to 0.2 (see Table 4), the ATS_1 values of the VSI DEWMA1-γ^2 chart and the VSI DEWMA2-γ^2 chart increases from 57.5901, 67.1396 up to 68.0586, 71.4070, respectively. These conclusions hold for the control charts when $ATS_0 = 500$.

It is noted that the above study is conducted based on the assumption that the parameter shift occurs at the beginning of the process monitoring, i.e. in the Zero-State (ZS) case. If the process has been running in an in-control state for some time, and the shift occurs in the process, it is the Steady-State (SS) case (see Ryan and Woodall [29]). Following the works of Xu and Jeske [30] and Dickinson et al. [31], it is assumed that in the SS case, the process is running in an in-control state for 50 samples and then the shift occurs. We investigate the SS performance of the VSI charts.

Table 6 presents the Adjusted ATSignal (AATS) values of the SS case of the VSI charts when $\gamma_0 = 0.1$ and $n = 5$. For a specific value of λ, the smallest value of $AATS_1$ for different τ in the VSI charts is in bold in the table. It is shown that, the VSI EWMA-γ^2 chart in SS performs best among these charts for large shifts and the VSI DEWMA2-γ^2 chart is superior to the other

Table 6. The out-of-control Adjusted Average Time to Signal (AATS) ($AATS_1$), values of various Variable Sampling Interval (VSI) charts for increases cases when $\gamma_0 = 0.1$ and $n = 5$.

λ	τ	**1.05**	**1.08**	**1.10**	**1.12**	**1.15**	**1.18**	**1.20**	**1.25**	**1.50**	**2.00**
0.10	VSI EWMA	91.0746	45.5990	30.2154	21.0919	13.2495	8.9948	**7.2202**	**4.5989**	**1.4136**	**0.4905**
	VSI DEWMA1	**60.3921**	29.6969	21.1553	16.1993	12.1892	9.8618	8.8053	7.1060	3.7595	1.9459
	VSI DEWMA2	61.1779	**29.3909**	**20.4626**	**15.1483**	**10.8486**	**8.4539**	7.3648	5.6552	2.5824	1.1433
	VSI DEWMA3	68.5451	33.9644	23.7140	17.9933	13.1741	10.4592	9.2859	7.2295	3.5385	1.7048
0.20	VSI EWMA	113.8994	61.4769	42.4689	30.1869	18.8121	12.4087	9.7017	5.7449	**1.3748**	**0.4429**
	VSI DEWMA1	**76.9907**	**36.7201**	**24.5892**	**17.3989**	11.5283	8.3840	7.0923	5.1609	2.2898	1.0439
	VSI DEWMA2	79.6286	38.7088	25.5754	18.0637	**11.5207**	**8.1680**	**6.7632**	**4.6364**	1.7562	0.7111
	VSI DEWMA3	84.9726	41.6101	27.8674	19.7102	12.9338	9.2441	7.7163	5.4755	2.2172	0.9250
0.25	VSI EWMA	123.4188	68.7978	47.9976	34.3315	21.5683	14.2629	11.2431	6.5320	**1.4161**	**0.4349**
	VSI DEWMA1	**84.5246**	**41.3294**	**27.2614**	**19.1632**	**12.3858**	**8.6253**	7.1349	4.9182	1.9583	0.8480
	VSI DEWMA2	87.6054	43.5631	29.1170	20.1394	12.7473	8.6901	**7.0780**	**4.6421**	1.5890	0.6214
	VSI DEWMA3	91.0804	45.5144	30.2638	21.1418	13.4416	9.3531	7.6966	5.2143	1.8888	0.7584
0.30	VSI EWMA	129.8890	74.1005	52.3781	37.8265	24.0815	16.0364	12.4682	7.2518	**1.4419**	**0.4289**
	VSI DEWMA1	**90.9465**	**45.2329**	**30.1411**	**20.9198**	**13.1452**	**9.0026**	**7.3322**	4.8140	1.7298	0.7116
	VSI DEWMA2	95.5391	48.7801	32.5730	22.6096	14.2004	9.5061	7.5724	**4.7578**	1.4935	0.5655
	VSI DEWMA3	99.1685	50.8235	34.0091	23.8584	14.9521	10.1086	8.1407	5.2615	1.7490	0.6656
0.50	VSI EWMA	150.0371	91.8886	67.3785	50.6816	33.6812	22.9612	18.1211	10.6150	1.7974	**0.4289**
	VSI DEWMA1	**115.7778**	**63.1778**	**43.7933**	**31.3301**	**19.5104**	**12.9844**	**10.1611**	**6.0308**	1.4310	0.4945
	VSI DEWMA2	119.5320	66.7318	46.5577	33.4153	21.0328	13.9706	10.9206	6.3888	**1.4005**	0.4507
	VSI DEWMA3	121.9752	67.7691	47.6245	33.9092	21.3555	14.2158	11.1971	6.5728	1.5084	0.4961

charts for moderate shifts. When it comes to small shifts, the VSI DEWMA1-γ^2 chart yields the smallest $AATS_1$. With the increase in λ, the advantage of the VSI DEWMA1-γ^2 chart in SS is more significant. For example, when λ increases from 0.1 up to 0.5, the range in which the VSI DEWMA1-γ^2 chart is better than the other VSI charts widens from $\tau \leq 1.05$ to $\tau \leq 1.25$.

4.5. Performance comparison of the proposed VSI DEWMA-γ^2 charts and the AEWMA-γ^2 chart

Haq and Khoo [9] proposed the AEWMA-γ^2 chart for monitoring the infrequent changes in the CV. For comparison, the ATS values of the VSI DEWMA-γ^2 charts and the AEWMA-γ^2 chart are presented in Table 7. It is observed that the VSI DEWMA-γ^2 charts always detect the shifts more quickly than the AEWMA-γ^2 chart. For example, when $\gamma_0 = 0.1$, the ATS_1 values of the AEWMA-γ^2 chart are 47.8 for $\tau = 1.1$, 1.5 for $\tau = 2$. By contrast, the ATS_1 values of the VSI DEWMA1-γ^2 chart are 17.6812 ($\tau = 1.1$) and 0.5389 ($\tau = 2$) when $\lambda = 0.1$, 43.9179 ($\tau = 1.1$) and 0.4102 ($\tau = 2$) when$\lambda = 0.5$. The ATS_1 values of the VSI DEWMA2-γ^2 chart are 23.6522 ($\tau = 1.1$) and 1.4281 ($\tau = 2$) when $\lambda = 0.1$, 47.3187 ($\tau = 1.1$) and 0.4738 ($\tau = 2$) for $\lambda = 0.5$. The values of the VSI DEWMA3-γ^2 chart are 15.6782 ($\tau = 1.1$) and 0.4045 ($\tau = 2$) when $\lambda = 0.1$, 47.5859 ($\tau = 1.1$) and 0.4472 ($\tau = 2$) when $\lambda = 0.5$. These facts show that the ATS_1 values of the VSI DEWMA-γ^2 charts with different λ are always smaller than the corresponding values of the AEWMA-γ^2 chart. The same conclusion holds for other values of γ_0.

5. A real application

To illustrate the implementation of the proposed VSI DEWMA-γ^2 charts, we consider a real industrial dataset from a sintering process and apply both the FSI charts and the VSI charts to analyze the dataset. This dataset was also used in Castagliola et al. [4] to illustrate the implementation of the EWMA-γ^2 charts.

In this real example, the properties related to the way atoms of a metal diffuse into one another in the sintering process often have a standard deviation that is proportional to the mean. Therefore, it is reasonable to monitor the process through CV. During the sintering process, the compressed metal powder is heated to a temperature that allows the bonding of the individual particles. The pore shrinking has a decisive effect on the strength of the bond between particles. One of the quality characteristics related to the pore shrinkage

Table 7. The out-of-control Average Time to Signal (ATS) (ATS_1), profiles of the Adaptive EWMA (AEWMA) and proposed charts for detecting increases in CV when $n = 5$ and $ATS_0 = 370.4$.

γ_0	τ	AEWMA	λ	0.10	0.20	0.25	0.30	0.50
0.05	1.10	47.4	VSI DEWMA1	16.4788	23.4094	26.3505	29.6942	43.0382
			VSI DEWMA2	23.0520	27.6231	30.4621	33.5739	47.4153
			VSI DEWMA3	15.7505	24.1732	28.8491	32.3040	46.8925
	1.25	9.1	VSI DEWMA1	2.8084	3.5442	3.8168	4.0980	5.6516
			VSI DEWMA2	6.4700	5.2287	5.0744	5.1309	6.6779
			VSI DEWMA3	2.1016	2.9434	3.5885	3.9143	6.3655
	1.50	3.1	VSI DEWMA1	0.9609	1.0997	1.1363	1.1604	1.2507
			VSI DEWMA2	2.9231	1.9566	1.7355	1.6116	1.4911
			VSI DEWMA3	0.7528	0.7472	0.8680	0.8910	1.4021
	2.00	1.5	VSI DEWMA1	0.4718	0.4311	0.4254	0.4127	0.3924
			VSI DEWMA2	1.2464	0.7538	0.6564	0.5885	0.4725
			VSI DEWMA3	0.4047	0.3094	0.3060	0.2949	0.4326
0.10	1.10	47.8	VSI DEWMA1	17.6812	23.9138	27.3367	30.2380	43.9179
			VSI DEWMA2	23.6522	27.4224	30.5953	33.6596	47.3187
			VSI DEWMA3	15.6782	24.8593	28.4360	32.6608	47.5859
	1.25	9.3	VSI DEWMA1	3.4683	3.9228	4.1088	4.2369	5.9160
			VSI DEWMA2	6.9658	5.3466	5.1658	5.2587	6.6687
			VSI DEWMA3	2.0337	2.9514	3.5116	3.9586	6.4822
	1.50	3.1	VSI DEWMA1	1.2254	1.2813	1.2767	1.2381	1.2933
			VSI DEWMA2	3.2688	2.0388	1.8082	1.6620	1.5029
			VSI DEWMA3	0.7495	0.7483	0.8419	0.8862	1.4235
	2.00	1.5	VSI DEWMA1	0.5389	0.4905	0.4712	0.4451	0.4102
			VSI DEWMA2	1.4281	0.7993	0.6833	0.6100	0.4738
			VSI DEWMA3	0.4045	0.3120	0.3063	0.2973	0.4472
0.15	1.10	48.4	VSI DEWMA1	21.5400	25.2155	28.1878	31.2911	44.9605
			VSI DEWMA2	25.3639	28.5717	31.3164	34.5354	48.9131
			VSI DEWMA3	15.6249	25.2904	29.1266	33.1808	46.9180
	1.25	9.4	VSI DEWMA1	5.8271	4.5711	4.5241	4.6455	6.0926
			VSI DEWMA2	8.1399	5.7953	5.4812	5.5021	6.9816
			VSI DEWMA3	2.0047	2.9604	3.5314	3.9800	5.9041
	1.50	3.2	VSI DEWMA1	2.4621	1.6164	1.4721	1.3971	1.3644
			VSI DEWMA2	3.9953	2.3047	1.9575	1.7832	1.5822
			VSI DEWMA3	0.7440	0.7483	0.8529	0.8964	1.0269
	2.00	1.6	VSI DEWMA1	1.0253	0.6142	0.5471	0.5008	0.4335
			VSI DEWMA2	1.8410	0.9156	0.7565	0.6704	0.5079
			VSI DEWMA3	0.4006	0.3126	0.3070	0.3010	0.2843
0.20	1.10	49.4	VSI DEWMA1	25.2254	26.7328	30.0313	32.1844	46.2760
			VSI DEWMA2	27.3714	29.2762	31.9915	36.0397	49.2641
			VSI DEWMA3	15.5223	25.5851	29.5266	33.5086	48.3863
	1.25	9.7	VSI DEWMA1	8.2235	5.4048	5.2182	4.9882	6.4788
			VSI DEWMA2	9.4548	6.2427	5.8688	5.9003	7.1492
			VSI DEWMA3	1.9375	2.9301	3.3263	4.0180	6.1759
	1.50	3.2	VSI DEWMA1	4.0079	2.0516	1.8177	1.5930	1.4777
			VSI DEWMA2	4.8706	2.6027	2.2057	1.9926	1.6485
			VSI DEWMA3	0.7405	0.7444	0.7627	0.8913	1.0748
	2.00	1.6	VSI DEWMA1	1.8460	0.8073	0.6948	0.5875	0.4768
			VSI DEWMA2	2.3560	1.0665	0.8701	0.7602	0.5403
			VSI DEWMA3	0.3986	0.3161	0.2966	0.3034	0.2929

is the pressure test drop time T_{pd} from 2 bar to 1.5 bar in more than 30 seconds. In Castagliola et al. [4], a regression study for the Phase I in-control samples showed that the standard deviation σ_{pd} of the pressure drop time T_{pd} is directly proportional to the mean μ_{pd}. Therefore, it is rational that the quality practitioners detect the shift in the process by monitoring the $\gamma_{pd} = \sigma_{pd}/\mu_{pd}$.

The Phase I dataset consists of $m = 20$ samples, each of size $n = 5$. The in-control $\hat{\gamma}_0$ is computed as $\hat{\gamma}_0 = \sum_{k=1}^{20} \hat{\gamma}_k/20 = 0.417$ by the root-mean-square estimation method, which has the advantages of high statistical efficiency, ease of computation and the availability of an explicit form. Values of the summary statistics $\bar{X}_k$, S_k, $\hat{\gamma}_0$, and $\hat{\gamma}_k^2$ of each sample are shown in the Table 8.

Based on the process engineers' knowledge, a shift of 25% (τ^*=1.25) in the CV indicates potential abnormalities in the production of the parts. In other words, a shift from $\hat{\gamma}_0 = 0.417$ to $\hat{\gamma}_1 = \hat{\gamma}_0 * 1.25 = 0.521$ indicates a tendency of being out-of-control. Considering the shift size 1.25 is moderate, the smoothing parameter $\lambda = 0.3$ is selected for illustration. We compute the K and W values of different VSI CV charts corresponding to the desired $ATS_0 = 370.4$, the sample size $n = 5$ and $(h_s, h_l) = (0.1, 1.9)$. The parameter combinations (λ, W, K) of the VSI CV charts are $(0.3, 0.4895, 5.4489)$ for the VSI EWMA-γ^2 chart, $(0.3, 0.6032, 4.1734)$ for the VSI DEWMA1-γ^2 chart, $(0.3, 0.6552, 4.1931)$ for the VSI DEWMA2-γ^2 chart, and $(0.3, 0.0800, 5.7398)$ for the VSI DEWMA3-γ^2 chart, respectively. The corresponding ATS_1 values are 11.1662, 8.3354, 8.6294 and 5.0256. By Eqs. (4) and (5), the warning and control limits (UWL, UCL) of the VSI EWMA-γ^2 chart are equal to $(0.1895, 0.5318)$. Similarly, the (UWL, UCL) of the VSI DEWMA1-γ^2 chart, the VSI DEWMA2-γ^2 chart, and VSI DEWMA3-γ^2 chart are $(0.1856, 0.3626)$, $(0.1882, 0.3636)$, $(0.0141, 1.0108)$, respectively. Note that it is assumed that the true value of γ_0 is unknown; hence the estimated $\hat{\gamma}_0$ is used for computing the *UWL*/*UCL* of all the control charts. The Phase I dataset was analyzed to be in-control using the SH-γ chart (see the corresponding figure in Castagliola et al. [4]). This is consistent with the conclusion by the proposed VSI methods. As shown in the last four columns of Table 8, the charting

Table 8. Phase I dataset from a sintering process.

					VSI EWMA	**VSI DEWMA1**	**VSI DEWMA2**	**VSI DEWMA3**
k	$\bar{X}_k$	S_k	$\hat{\gamma}_k$	$\hat{\gamma}_k^2$	Z_k	Z_k	Z_k	Z_k
1	664.2	268.9	0.405	0.1640	0.1582	0.1565	0.1565	–0.0314
2	705.6	308.6	0.437	0.1910	0.1681	0.1600	0.1600	–0.0605
3	1051.5	539.9	0.513	0.2632	0.1966	0.1710	0.1710	–0.0464
4	1047.3	359.0	0.343	0.1176	0.1729	0.1715	0.1715	–0.0712
5	618.2	136.3	0.221	0.0488	0.1557	0.1608	0.1608	–0.1129
6	781.4	446.4	0.571	0.3260	0.2068	0.1704	0.1704	–0.0658
7	797.8	342.5	0.429	0.1840	0.2000	0.1763	0.1763	–0.0572
8	678.9	275.4	0.406	0.1648	0.1894	0.1782	0.1782	–0.0788
9	848.3	320.5	0.378	0.1429	0.1755	0.1759	0.1759	–0.1182
10	1015.3	453.7	0.447	0.1998	0.1828	0.1770	0.1770	–0.1386
11	777.4	276.4	0.356	0.1267	0.1659	0.1729	0.1729	–0.1721
12	813.9	170.7	0.210	0.0441	0.1557	0.1594	0.1594	–0.2089
13	716.6	397.4	0.554	0.3069	0.2011	0.1660	0.1660	–0.1612
14	937.6	421.2	0.449	0.2016	0.2012	0.1725	0.1725	–0.1342
15	915.1	331.9	0.363	0.1318	0.1804	0.1720	0.1720	–0.1447
16	873.2	285.0	0.326	0.1063	0.1582	0.1658	0.1658	–0.1728
17	984.3	573.7	0.583	0.3399	0.2127	0.1785	0.1785	–0.1060
18	819.3	156.2	0.191	0.0365	0.1598	0.1719	0.1719	–0.0997
19	839.0	244.0	0.291	0.0847	0.1557	0.1608	0.1608	–0.1235
20	585.8	322.3	0.550	0.3025	0.1998	0.1681	0.1681	–0.0796

statistic Z_k falls below the *UCLs* of the VSI charts, indicating the sintering process is in-control. Based on all the Phase I data, we obtain the estimate $\hat{\gamma}_0 = 0.417$ and set the control limits for Phase II control charts accordingly.

In Phase II monitoring, the 20 samples and the values of charting statistics of the proposed VSI CV charts are presented in Table 9. Here Z_k represents the value of the charting statistic at the kth sample and t_k denotes the cumulative time until the kth sample. The different CV charts are plotted in Figure 2 for comparison, where Figure 2(a)-(d) are the FSI CV charts and Figure 2(e)-(g) are the corresponding VSI CV charts.

From Figure 2(a) and (e), it is noted that the FSI EWMA-γ^2 chart and the VSI EWMA-γ^2 chart fail to detect the shift. The FSI DEWMA1-γ^2 chart and the FSI DEWMA2-γ^2 chart in Figure 2(b) and (c) give an out-of-control signal at the 8th sample (corresponding to the bolded values in Table 9), which means the two FSI charts take 8 time units to detect the assignable cause. The FSI DEWMA3-γ^2 chart in Figure 2(d) takes 14 time units to detect the shift. This fact indicates that the FSI DEWMA1-γ^2 chart and the FSI DEWMA2-γ^2 chart detect the shift faster than the FSI DEWMA3-γ^2 chart.

Moreover, from the comparison of Figure 2(b)-(d) and (f)-(h), it can be noted that the VSI DEWMA-γ^2 charts always outperform the corresponding FSI DEWMA-γ^2 charts. For the VSI DEWMA1- γ^2 chart and the VSI DEWMA2-γ^2 chart in Figure 2(f) and (g), both the first charting statistics Z_1 fall in the central region, which result in a large sampling interval $h_l = 1.9$ to obtain the second sample; and both charts spend 2.6 time units to detect the shift. For the VSI DEWMA3-γ^2 chart in Figure 2(h), it only takes 1.4 time units to detect the shift, which is faster than the VSI DEWMA1- γ^2 chart and the VSI DEWMA2-γ^2 chart. When the signal is triggered, some remedial actions should be taken as soon as possible to find and eliminate the special causes in the manufacturing process.

6. Conclusions

In this paper, we have proposed three Double Exponentially Weighted Moving Average (DEWMA) charts with Variable Sampling Interval (VSI) features to monitor the Coefficient of Variation (CV) squared. Depending on the position of the previously plotted points on the chart, the proposed VSI DEWMA-γ^2 charts allow the sampling interval to vary between two

Table 9. Phase II dataset from a sintering process.

				VSI EWMA		VSI DEWMA1		VSI DEWMA2		VSI DEWMA3	
k	$\bar{X}_k$	S_k	$\hat{\gamma}_k^2$	Z_k	t_k	Z_k	t_k	Z_k	t_k	Z_k	t_k
1	906.4	476.0	0.2756	0.1917	0.1	0.1665	0.1	0.1665	0.1	0.0297	0.1
2	805.1	493.9	0.3770	0.2473	0.2	0.1908	2.0	0.1908	2.0	0.1269	0.2
3	1187.2	1105.9	0.8686	0.4337	0.3	0.2636	2.1	0.2636	2.1	0.5177	0.3
4	663.4	304.8	0.2107	0.3668	0.4	0.2946	2.2	0.2946	2.2	0.6568	0.4
5	1012.1	367.4	0.1318	0.2963	0.5	0.2951	2.3	0.2951	2.3	0.6299	0.5
6	863.2	350.4	0.1648	0.2568	0.6	0.2836	2.4	0.2836	2.4	0.5291	0.6
7	1561.0	1652.2	1.1194	0.5156	0.7	0.3532	2.5	0.3532	2.5	0.9240	0.7
8	697.1	253.2	0.1318	0.4005	0.8	**0.3674**	**2.6**	**0.3674**	**2.6**	0.9985	0.8
9	1024.6	120.9	0.0139	0.2845	0.9	0.3425	2.7	0.3425	2.7	0.9092	0.9
10	355.3	235.2	0.4382	0.3306	1.0	0.3389	2.8	0.3389	2.8	0.9024	1.0
11	485.6	106.5	0.0480	0.2458	1.1	0.3110	2.9	0.3110	2.9	0.7820	1.1
12	1224.3	915.4	0.5595	0.3399	1.2	0.3197	3.0	0.3197	3.0	0.8378	1.2
13	1365.0	1051.6	0.5929	0.4158	1.3	0.3485	3.1	0.3485	3.1	0.9934	1.3
14	704.0	449.7	0.4083	0.4136	1.4	0.3680	3.2	0.3680	3.2	**1.0826**	**1.4**
15	1584.7	1050.8	0.4396	0.4214	1.5	0.3840	3.3	0.3840	3.3	1.1485	1.5
16	1130.0	680.6	0.3624	0.4037	1.6	0.3899	3.4	0.3899	3.4	1.1547	1.6
17	824.7	393.5	0.2275	0.3508	1.7	0.3782	3.5	0.3782	3.5	1.0572	1.7
18	921.2	391.6	0.1806	0.2998	1.8	0.3547	3.6	0.3547	3.6	0.8920	1.8
19	870.3	730.0	0.7039	0.4210	1.9	0.3746	3.7	0.3746	3.7	0.9951	1.9
20	1068.3	150.8	0.0199	0.3007	2.0	0.3524	3.8	0.3524	3.8	0.9202	2.0

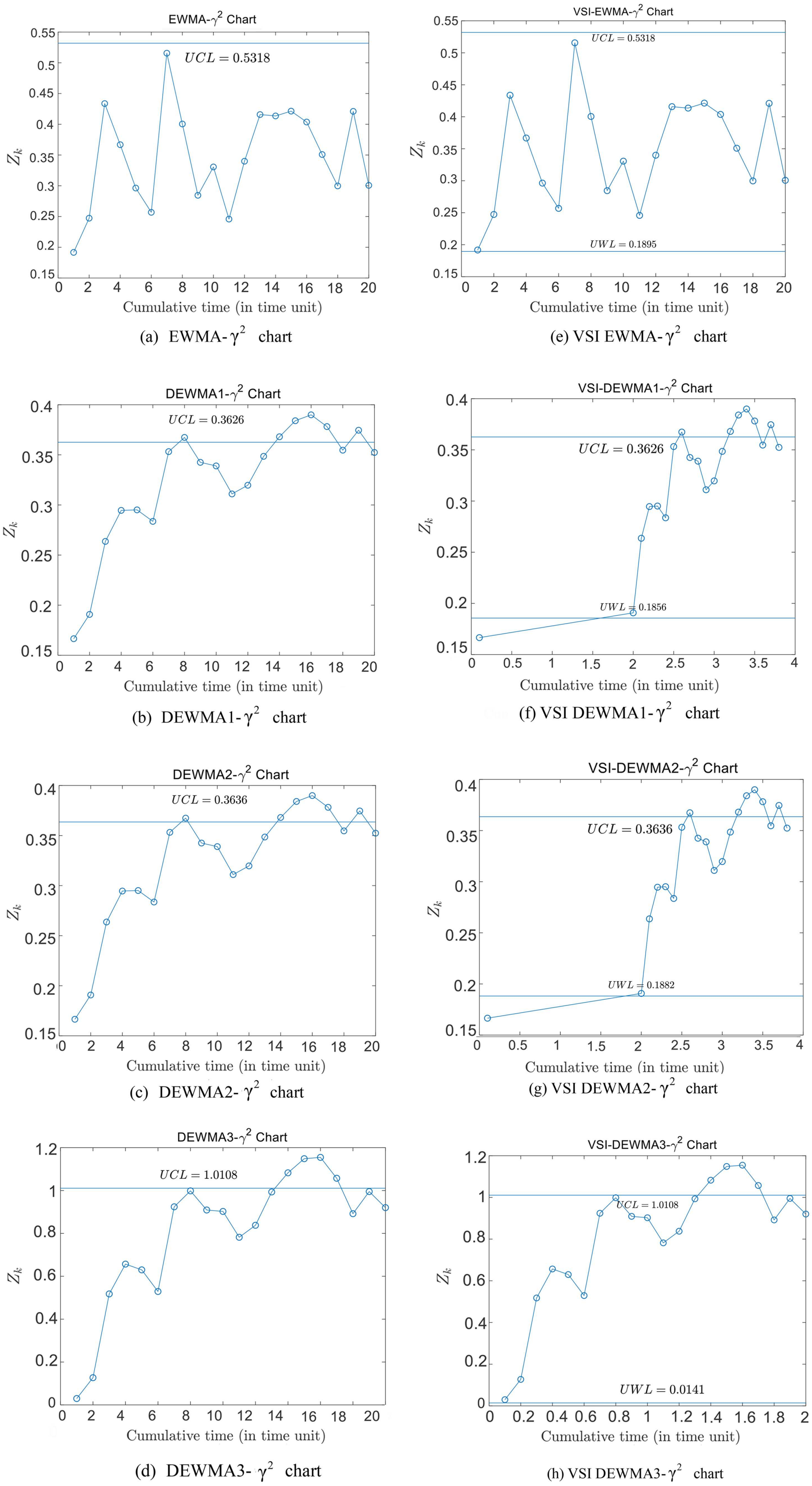

Figure 2. Fixed Sampling Interval (FSI) and Variable Sampling Interval (VSI) Coefficient of Variation (CV) charts applied to the sintering process.

samples. The Average Time to Signal (ATS) of the proposed control charts is computed using Monte Carlo simulation method. The comparisons of the Fixed Sampling Interval (FSI DEWMA-γ^2) charts and the VSI EWMA-γ^2 charts show the outperformance of the VSI DEWMA-γ^2. In addition, the VSI DEWMA1-γ^2 chart and the VSI DEWMA3-γ^2 are highly recommended when a large smoothing parameter or a large in-control γ_0 is chosen. Finally, the implementation of the proposed VSI DEWMA-γ^2 charts is demonstrated for a better use of the charts by the practitioners.

The proposed CV charts are constructed based on the assumption that each observation follows a normal distribution, which is a restrictive requirement. In many applications, however, the underlying distribution for the process is non-normal. The violation of the normality assumption may have tremendous adverse effect on the CV charts. Hence, it is of great value to study the CV charts when the underlying distribution is unknown or non-normal. Moreover, monitoring the multivariate CV is another valuable and interesting topic.

Declaration of Conflicting Interests

There are no relevant financial or non-financial competing interests to report.

Funding

The author(s) disclosed receipt of the following financial support for the research, authorship, and/or publication of this article: This work was supported by National Natural Science Foundation of China [grant number 71802110, 71872088], Postgraduate Research and Practice Innovation Program of Jiangsu Province[grant number KYCX21_0840], Key Research Base of Philosophy and Social Sciences in Jiangsu-Information Industry Integration Innovation and Emergency Management Research Center, the Excellent Innovation Teams of Philosophy and Social Science in Jiangsu Province [grant number 2017ZSTD022].

References

1. Yeong, W.C., Khoo, M.B.C., Tham, L.K., et al. "Monitoring the coefficient of variation using a variable sampling interval EWMA chart", *Journal of Quality Technology*, **49**(4), pp. 380–401 (2017). DOI: 10.1080/00224065.2017.11918004

2. Kang, C.W., Lee, M.S., Seong, Y.J., et al. "A control chart for the coefficient of variation", *Journal of Quality Technology*, **39**(2), pp. 151–158 (2007). DOI: 10.1080/00224065.2007.11917682

3. Hong, E.-P., Kang ,C.-W., Baek, J.-W., et al. "Development of CV control chart using EWMA technique", *Journal of the Society of Korea Industrial and Systems Engineering*, **31**(4), pp. 114–120 (2008).

4. Castagliola, P., Celano, G., and Psarakis, S. "Monitoring the coefficient of variation using EWMA charts", *Journal of Quality Technology*, **43**(3), pp. 249–265 (2011). DOI: 10.1080/00224065.2011.11917861

5. Calzada, M.E. and Scariano, S.M. "A synthetic control chart for the coefficient of variation", *Journal of Statistical Computation and Simulation*, **83**(5), pp. 853–867 (2013). DOI: 10.1080/00949655.2011.639772

6. Zhang, J., Li, Z., Chen, B., et al. "A new exponentially weighted moving average control chart for monitoring the coefficient of variation", *Computers and Industrial Engineering*, **78**, pp. 205–212 (2014). https://doi.org/10.1016/j.cie.2014.09.027

7. Zhang, J., Li, Z., and Wang, Z. "Control chart for monitoring the coefficient of variation with an exponentially weighted moving average procedure", *Quality and Reliability Engineering International*, **34**(2), pp. 188–202 (2018). https://doi.org/10.1002/qre.2247

8. Shu, L. and Jiang, W. "A new EWMA chart for monitoring process dispersion", *Journal of Quality Technology*, **40**(3), pp. 319–331 (2008). DOI: 10.1080/00224065.2008.11917737

9. Haq, A. and Khoo, M.B.C. "New adaptive EWMA control charts for monitoring univariate and multivariate coefficient of variation", *Computers and Industrial Engineering*, **131**, pp. 28–40 (2019). https://doi.org/10.1016/j.cie.2019.03.027

10. Castagliola, P., Achouri, A., Taleb, H., et al. "Monitoring the coefficient of variation using control charts with run rules", *Quality Technology and Quantitative Management*, **10**(1), pp. 75–94 (2013). DOI: 10.1080/16843703.2013.11673309

11. Chen, R., Li, Z., and Zhang, J. "A generally weighted moving average control chart for monitoring the coefficient of variation", *Applied Mathematical Modelling*, **70**, pp. 190–205 (2019). https://doi.org/10.1016/j.apm.2019.01.034

12. Teoh, W.L., Khoo, M.B.C., Castagliola, P., et al. "Run–sum control charts for monitoring the coefficient of variation", *European Journal of Operational Research*, **257**(1), pp. 144–158 (2017). https://doi.org/10.1016/j.ejor.2016.08.067

13. Hu, X., Zhang, S., Zhou, X., et al. "The performance of double exponentially weighted moving average control charts for monitoring the coefficient of variation", *Communications in Statistics-Simulation and Computation*, **53**(4), pp. 1–20 (2022). DOI: 10.1080/03610918.2022.2057539

14. Jalilibal, Z., Amiri, A., Castagliola, P., et al. "Monitoring the coefficient of variation: A literature review", *Computers and Industrial Engineering*, p. 107600 (2021). https://doi.org/10.1016/j.cie.2021.107600

15. Saccucci, M.S., Amin, R.W., and Lucas, J.M. "Exponentially weighted moving average control schemes with variable sampling intervals", *Communications in Statistics - Simulation and Computation*, **21**(3), pp. 627–657 (1992). DOI: 10.1080/03610919208813040

16. Shamma, S.E., Amin, R.W, Shamma AK. "A double exponentially weigiited moving average control procedure with variable sampling intervals", *Communications in Statistics - Simulation and Computation*, **20**(2–3), pp. 511–528 (1991). DOI: 10.1080/03610919208813040

17. Castagliola, P., Celano, G., Fichera, S., et al. "A variable sample size S2-EWMA control chart for monitoring the process variance", *International Journal of Reliability, Quality and Safety Engineering*, **15**(03), pp. 181–201 (2008). DOI: 10.1142/s0218539308003039

18. Haq, A. and Akhtar, S. "Auxiliary information based maximum EWMA and DEWMA charts with variable sampling intervals for process mean and variance", *Communications in Statistics - Theory and Methods*, **51**(12), pp. 3985–4005 (2020). DOI: 10.1080/03610926.2020.1805766

19. Reynolds, M.R., Amin, R.W., and Arnold, J.C. "CUSUM charts with variable sampling intervals", *Technometrics*, **32**(4), pp. 371-384 (1990). DOI: 10.2307/1270114

20. Reynolds, M.R. and Arnold, J.C. "EWMA control charts with variable sample sizes and variable sampling intervals", *IIE Transactions*, **33**(6), pp. 511–530 (2001). DOI: 10.1080/00224065.2001.11980048

21. Castagliola, P., Achouri, A., Taleb, H., et al. "Monitoring the coefficient of variation using a variable sampling interval control chart", *Quality and Reliability Engineering International*, **29**(8), pp. 1135–1149 (2013). https://doi.org/10.1002/qre.1465

22. Khaw, K.W., Khoo, M.B.C., Yeong, W.C., et al. "Monitoring the coefficient of variation using a variable sample size and sampling interval control chart", *Communications in Statistics - Simulation and Computation*, **46**(7), pp. 5772–5794 (2017). DOI: 10.1080/03610918.2016.1177074

23. Muhammad, A.N.B., Yeong, W.C., Chong, Z.L., et al. "Monitoring the coefficient of variation using a variable sample size EWMA chart", *Computers and Industrial Engineering*, **126**, pp. 378–398 (2018). https://doi.org/10.1016/j.cie.2018.09.045

24. Nguyen, H.D., Nguyen, Q.T., Tran, K.P., et al. "On the performance of VSI Shewhart control chart for monitoring the coefficient of variation in the presence of measurement errors", *The International Journal of Advanced Manufacturing Technology*, **104**(1), pp. 211–243 (2019). DOI: 10.1007/s00170-019-03352-7

25. Tran, P.H. and Heuchenne, C. "Monitoring the coefficient of variation using variable sampling interval CUSUM control charts", *Journal of Statistical Computation and Simulation*, **91**(3), pp. 501–521 (2021). DOI: 10.1080/00949655.2020.1819278

26. Breunig, R. "An almost unbiased estimator of the coefficient of variation", *Economics Letters*, **70**(1), pp. 15–19 (2001). https://doi.org/10.1016/S0165-1765(00)00351-7

27. Shamma, S.E. and Shamma, A.K. "Development and evaluation of control charts using double exponentially weighted moving averages", *International Journal of Quality and Reliability Management*, **9**(6) (1992). DOI: 10.1108/02656719210018570

28. Hamilton, M.D. and Crowder, S.V. "Average run lengths of EWMA control charts for monitoring a process standard deviation", *Journal of Quality Technology*, **24**(1), pp. 44–50 (1992). DOI: 10.1080/00224065.1992.11979373

29. Ryan, A.G. and Woodall, W.H. "Control charts for poisson count data with varying sample sizes", *Journal of Quality Technology*, **42**(3), pp. 260-275 (2010). DOI: 10.1080/00224065.2010.11917823

30. Xu, S. and Jeske, D.R. "Weighted EWMA charts for monitoring type I censored Weibull lifetimes", *Journal of Quality Technology*, **50**(2), pp. 220–230 (2018). DOI: 10.1080/00224065.2018.1436830

31. Dickinson, R.M., Roberts, D.A.O, Driscoll, A.R., et al. "CUSUM charts for monitoring the characteristic life of censored Weibull lifetimes", *Journal of Quality Technology*, **46**(4), pp. 340–358 (2014). DOI: 10.1080/00224065.2014.11917976

32. Qiu, P. and Li, Z. "Distribution-free monitoring of univariate processes", *Statistics and Probability Letters*, **81**(12), pp. 1833–1840 (2011).

Biographies

Xuelong Hu is currently an Associate Professor at Nanjing University of Posts and Telecommunications, Nanjing, China. His research activity includes new SPC techniques and has published many research articles on control charts, especially on control charts with estimated parameters, control charts with measurement errors and time between events control charts.

Suying Zhang is currently MSc student of the School of Management at Nanjing University of Posts and Telecommunications, Nanjing, China. His research focuses on statistical quality control.

Yang Zhang is an Associate Professor in the School of Management at Tian University of Commerce, China. He received his PhD degree in the industrial engineering from Tianjin University, China, in 2013. His current research interests focused on quality engineering and service quality management.

Jiujun Zhang is a Professor of Department of Mathematics, Liaoning University, China. He obtained his BSc, MSc degrees in statistics from Liaoning Normal

University and PhD degree in statistics from Nankai University, China. His research interests include statistical process control, applied statistics, and related applications. His research has been published in various refereed journals including Quality and Reliability Engineering International, European Journal of Operational Research, International Journal of Advanced Manufacturing Technology, and Computers and Industrial Engineering.

Panpan Zhou is an Assistant Professor at Nanjing University of Finance and Economics, China. Her research interests mainly focus on quality engineering, statistical process control, and design of experiments.